Available online at www.sciencedirect.com
ScienceDirect
C. R. Chimie 11 (2008) 159–182
COMPTES RENDUS CHIMIE
http://france.elsevier.com/direct/CRAS2C/

Account / Revue

Synthetic approaches to the molybdenum sulfide materials

Pavel Afanasiev

Institut de recherches sur la catalyse et l'environnement, 2, avenue Albert-Einstein, 69626 Villeurbanne cedex, France

Received 16 January 2007; accepted after revision 24 April 2007
Available online 2 July 2007

Abstract

Synthetic aspects of the molybdenum sulfide-based materials were reviewed, with emphasis on the catalytic materials. A number of preparation methods were critically compared in this review, including molecular precursor decomposition, hydrothermal, soft chemistry aqueous, surfactant-aided, intercalation–exfoliation, and solid–gas reactions. In particular, the relationship between the preparation techniques and the properties of the materials obtained was analyzed. Preparation of bulk Co–Mo–S and Ni–Mo–S mixed sulfides based on the MoS_2 structure and eminently important for catalysis was also considered. ***To cite this article: P. Afanasiev, C. R. Chimie 11 (2008).***

Résumé

Des aspects synthétiques des matériaux à base de sulfure de molybdène ont été considérés, en insistant sur les matériaux catalytiques. Un certain nombre de méthodes de préparation ont été comparées dans cette revue, y compris la décomposition des précurseurs, les synthèses hydrothermales, les synthèses en solution par méthodes de chimie douce, les préparations en présence de tensioactifs, l'intercalation–exfoliation, et les réactions gaz–solide. En particulier, la relation entre les techniques de préparation et les propriétés des matériaux obtenus a été analysée. La préparation des solides Co–Mo–S et Ni–Mo–S basés sur la structure MoS_2 et éminemment importants pour la catalyse a été également considérée. ***Pour citer cet article : P. Afanasiev, C. R. Chimie 11 (2008).***

Keywords: Molybdenum; Sulfide; Catalysts; Preparation

Mots-clés : Molybdène ; Sulfure ; Catalyseurs ; Préparation

1. Introduction

Molybdenum is one of the essential elements in modern technology. It is also a crucial microelement in living organisms, including humans. All molybdenum enzymes contain sulfur [1–5]. Many sulfur-containing molybdenum complexes were synthesized and structurally characterized [6,7]. Within the various thiomolybdate anions, the molybdenum ions are found in different oxidation states (IV, V, and VI), and they are bound by sulfide and polysulfide ligands in various coordination modes. A close matching of the S 3p and Mo 4d orbital energies makes easy an internal electron transfer. As a result, the sulfur–molybdenum cores display an extraordinary intramolecular lability. In other words, rearrangements are easily possible where S–S bonds

E-mail address: afanas@catalyse.univ-lyon1.fr

1631-0748/$ - see front matter
doi:10.1016/j.crci.2007.04.009

break or form as Mo atoms are oxidized or reduced, leading to the existence of versatile structural isomers.

Synthetic aspects of molecular sulfur-containing coordination compounds were extensively reviewed earlier [8]. The topic of the present review is narrower: it deals with the synthesis and properties of molybdenum sulfides for the goals of materials chemistry. By far the most studied among the molybdenum sulfides is MoS_2, which finds practical applications in diverse areas. A number of methods is considered in this review, including molecular precursor decomposition, hydrothermal, soft chemistry aqueous, surfactant-aided, ultrasonically assisted, intercalation–exfoliation, and solid–gas reactions. The important part of this review considers various synthetic routes to MoS_2 and the properties of the as obtained materials. Though this review is mostly devoted to the MoS_2-based materials, all known molybdenum sulfides are briefly described. Bulk Co–Mo–S and Ni–Mo–S mixed sulfides based on the MoS_2 structure and eminently important for catalysis will be also considered when relevant. Though even more important, supported MoS_2 materials (heterogeneous hydrotreating catalysts) will only be marginally mentioned here.

2. Known molybdenum sulfides

Stable oxidation states of molybdenum range from 0 to VI. As for sulfur in the inorganic sulfides, it is commonly present as S^{2-} or S_2^{2-} species. From the sulfides so imaginable, only Mo(V), Mo(IV), Mo(III) and Mo(II) ones were described with more or less certitude (while only the Mo(IV) one is important for chemistry and industry). Oxidizing properties of Mo(VI) make impossible its coexistence with the S^{2-} ion in the neutral species. By contrast, the total electronegativity might be reduced by addition of a negative charge and the Mo(VI) thioanions MoS_4^{2-} are relatively stable in the ionic salts and in aqueous solutions. However, if the corresponding MoS_3 sulfide is isolated, intramolecular oxidation of the sulfide ions and reduction of molybdenum to lower oxidation states (V or IV) occur. The sulfides having oxidation state of molybdenum lower than (II) were never described. The analogy with the corresponding suboxides (such as Mo_3O) probably fails here, because of the larger size of sulfide anion, which cannot fill the interstices of the metal structure.

2.1. Molybdenum sulfides with Mo oxidation state lower than IV

Several sulfides with lower formal oxidation states of molybdenum have been characterized. These compounds are usually prepared by high-temperature reactions including elements and simple compounds in sealed quartz tubes. Considerable part of these works came from the Sergent and Chevrel group.

Chevrel phase-related trigonal (*R*-3*R*) Mo_6S_8 was prepared in Refs. [9,10]. Its structure is characterized by a Mo_6S_8 motif containing octahedral Mo_6 clusters (Mo–Mo = 2.69 and 2.86 Å) inserted into a distorted cube of sulfur atoms. The related sulfide obtained by self-intercalation of molybdenum into Mo_6S_8 host is $Mo_{1.18}Mo_6S_8$ or $Mo_{7.18}S_8$ [11]. Mo_6S_8 is a generic host for different derivatives, so-called Chevrel phases which can be considered as products of intercalation of different chemical species (particularly bivalent cations such as Pb^{2+}) between the Mo_6S_8 units. Many compounds of this family were studied in relation to their superconductivity, for example the products of stabilization of Mo_6S_8 by halogens $Mo_6S_6Br_2$ and $Mo_6S_6I_2$ [12].

Besides Chevrel phase-related sulfides, several other compounds are known: monoclinic dimolybdenum trisulfide Mo_2S_3 was obtained by Khlybov et al. [13]. Its structure was resolved and high-pressure transition described. Mo_2S_3 has a monoclinic *P*2/*m* structure with a metallic character. The Mo and S atoms build some complex columns of MoS_6 octahedral which host large rectangular void spaces [14]. Electronic properties and phase transitions in the Mo-chain compound Mo_2S_3 were studied in Ref. [15]. The results of electrical resistivity, magnetic susceptibility, and Raman scattering measurements were presented. Phase transitions are observed in this material at temperatures of 182 and 145 K on cooling from room temperature.

Another sulfide of $Mo_{15}S_{19}$ stoichiometry was obtained by Tarascon and Hull [16] together with a sequence of several ternary molybdenum sulfide phases $M_{3.4}Mo_{15}S_{19}$ (M = vacancy, Li, Na, K, Zn, Cd, Sn and Tl). First the $In_{3.4}Mo_{15}S_{19}$, was obtained, and then it was shown that indium atoms can be removed from this phase by oxidation with HCl without disturbing the Mo chalcogenide network, resulting in a new binary phase $Mo_{15}S_{19}$. Furthermore, this phase, with an open framework structure turns out to be an interesting system for intercalation studies.

Despite their interesting properties and sometimes fascinating structures, the studies of these sulfur-deficient sulfides still mostly belong to the field of exploratory solid-state chemistry.

2.2. Amorphous sulfur-rich sulfides: MoS_3, MoS_4 and beyond

Several stoichiometric sulfur-rich sulfides were described. None of them was obtained in crystalline

form. In all of them molybdenum should be considered as having an intermediate oxidation state close to V.

The amorphous MoS_3 compound can be obtained either by aqueous hydrolysis of MoS_4^{2-} species or by gentle decomposition of $(NH_4)_2MoS_4$. MoS_3 was first prepared by Yagoda and Fales by acidification of a thiomolybdate solution [17]:

$$MoS_4^{2-} + 2H^+ = MoS_3 + H_2S \quad (1)$$

Alternatively it can be prepared by decomposing ammonium thiomolybdate salt at moderate temperature:

$$(NH_4)_2MoS_4 = MoS_3 + 2NH_3 + H_2S \quad (2)$$

The last one above 673 K further decomposes to MoS_2:

$$MoS_3 = MoS_2 + 1/8S_8 \quad (3)$$

MoS_3 can also be obtained by anodic oxidation of thiomolybdate [18].

The possible involvement of amorphous MoS_3 in the hydrodesulfurisation catalysts [19] and its potential use as a cathode material [20] motivated several research groups to study it by diffraction [21–23] and extended X-ray absorption fine structure (EXAFS) [24–27]. Other techniques were also applied, including chemical extrusion [28], vibrational and photoelectron spectroscopy [29]. However, the structure of this amorphous material appeared to be difficult to elucidate. The presence of abundant S–S bridges binding together the Mo atoms in this amorphous solid was obvious; however, the mode of their arrangement was questionable. Few physical methods are suitable to study this type of solids. Those providing direct structural information are only EXAFS and neutrons diffraction. Some studies concluded that MoS_3 is made up of disordered chains [23], but others postulated that it is built from Mo_3 triangles [29].

Finally Hibble et al. provided the structural evidence from the modeling of the neutron diffraction data obtained for amorphous MoS_3 [30]. This work demonstrated that the material is built from MoS_6 octahedral linked by face sharing to form Mo_2S_9 units containing metal–metal bonded dimers. These units are linked by sharing the remaining octahedral faces of the MoS_6 units to form extended chains (Fig. 1).

With respect to this discussion, note that the structure of MoS_3 obtained by various methods might be different, since polymorphism and isomerism in the Mo–S structures are well known. At least there is no reason why chain-like and trimeric MoS_3 could not coexist.

Among the sulfur-rich molybdenum sulfides, MoS_3 is the most studied one because its formation was supposed

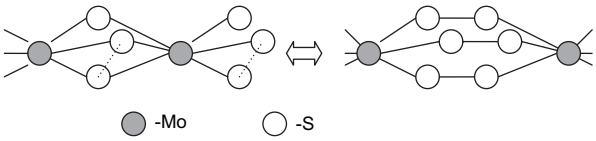

Fig. 1. Supposed chain structure of MoS_3 and its extension up to MoS_6 by adding new S–S bridges.

in the hydrotreating catalysts during activation. Some authors claim that MoS_3 is an intermediate product of the oxide sulfidation to MoS_2 [31,32]. Whatever the truth about the sulfidation of oxides, MoS_3 is surely the intermediate product of MoS_2 syntheses from thiomolybdate. As such, MoS_3 is easy to confuse with poorly crystallized substoichiometric MoS_{2+x}, containing small fringes with abundant S_2^{2-} groups at the edges. Indeed, both sulfides give broad XRD lines at similar 2θ angles. That is expected since, for a poorly crystalline solids, the XDR pattern reveals radial distribution function (RDF) which is similar in two solids; RDF is constituted from Mo–S, S–S and Mo–Mo distances. To check which sulfide is really present, ESR spectroscopy might be helpful. MoS_2 as such is ESR-silent, but only the edge-located Mo(V) sites give a strong paramagnetic signal. Next, trigonal prismatic Mo(V) in MoS_2 gives a simple axial signal with $g_\perp > g_\parallel$ (Fig. 2a), whereas MoS_3 shows a more complex signal extending to smaller g factors, suggesting that molybdenum coordination is close to the distorted octahedral (Fig. 2b). Electron-spin resonance of paramagnetic species was applied as a tool for studying the thermal decomposition of molybdenum trisulfide [33]. Paramagnetic species were observed attributed to MoS_3^+ species, whose magnetic parameters were different depending on which phase, either MoS_3 or MoS_2, was predominant.

2.2.1. MoS_4, MoS_5, MoS_6

These are all amorphous compounds without clear chemical identity. Since no crystalline sulfides with S/Mo ratio greater than 2 exist on the phase diagram Mo–S, their preparations are all soft chemistry ones and often carried out using sulfur-rich thiomolybdates.

Rice et al. prepared sulfur-rich sulfides of Cr, Mo and W by the reaction of $M(CO)_6$ (M = Cr, Mo, W) with sulfur in 1,2 dichlorobenzene [34]. Amorphous MoS_4 compound was obtained by this route. The solid was characterized by IR spectroscopy and demonstrated a broad band at 516 cm^{-1}, close to what was expected for a compound with abundant S–S bonds. Its decomposition as studied by DSC led to the MoS_2.

Khudorozhko et al. prepared MoS_4 sulfide by means of thiodimolybdate decomposition at moderate

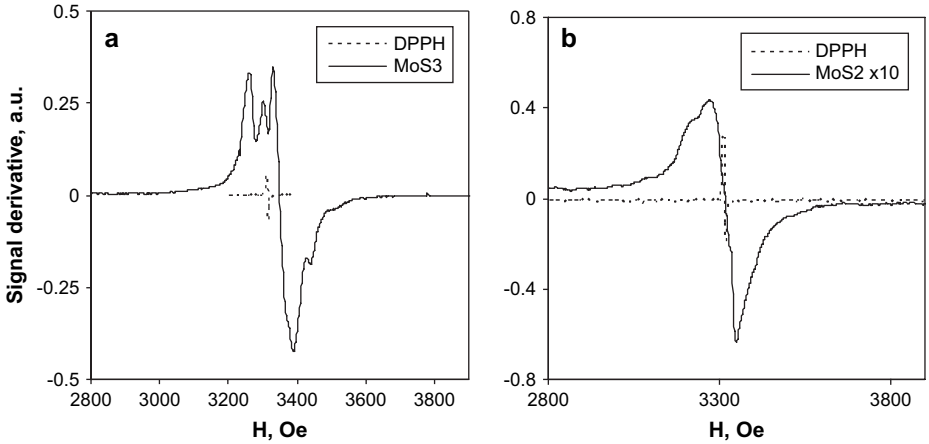

Fig. 2. X band ESR spectra of MoS_3 dried under nitrogen (a) and poorly crystalline MoS_2 (b) obtained from the decomposition of thiomolybdate at 350 °C. Spectra are measured at −196 °C (liquid nitrogen).

temperatures [35]. An X-ray amorphous phase with the analytical formula MoS_4 was synthesized. The authors claimed rather by analogy that the structure of this compound is similar to that of chain-like VS_4 sulfide. The electronic structure of molybdenum tetrasulfide and its lithium intercalates has been studied by X-ray emission and X-ray electron spectroscopies. The change of electronic structure of initial molybdenum tetrasulfide under intercalation of up to four lithium atoms per formula unit was interpreted on the basis of the rigid-band model. Further intercalation of up to seven atoms per formula unit probably leads to a destructive change of the one-dimensional structure of the matrix.

Recently we prepared stoichiometric compounds by oxidation or acid condensation of thiodimolybdate [36]:

$$Mo_2S_{12}^{2-} + 2H^+ = Mo_2S_{11} + H_2S \quad (4)$$

$$Mo_2S_{12}^{2-} + 2I^- = 2MoS_6 + I_2 \quad (5)$$

The structure of these solids seems be related to MoS_3, because their XRD patterns and EXAFS spectra show much similarity. From the great mobility of Mo–S bonds and relative stability of the S–S bridges, it follows that new S–S bonds can be easily inserted within the chains of MoS_3 (Fig. 1). Since MoS_3 is amorphous, no structural hindrances would exist for such chain extensions, and we should be able to synthesize MoS_x solids in the whole range of x from 3 to at least 6 (and even more, because S_4^{2-} entities are also common in thiomolybdates). Presumably, other stoichiometric sulfides can be produced from the solutions of other thiomolybdates by means of similar techniques. Their properties are expected to be close to those of the described sulfur-rich sulfides.

2.3. MoS_2

MoS_2 is the molybdenum sulfide by far the most studied in materials chemistry. It constitutes the main active component of the existing hydrotreating supported catalysts [37]. The second main application of MoS_2 is related to its tribological properties [38]. The emerging class of new highly loaded sulfide catalysts contain an almost pure molybdenum sulfide phase promoted with cobalt or nickel as a bulk compound, mixed with some small amounts of binders and/or textural promoters. Considerable research effort was dedicated to the synthesis of high surface area molybdenum sulfide materials. At the same time particular morphologies of this compound such as tubular, hollow spherical and other are actively searched, using various chemical approaches.

The MoS_2 compound is thermodynamically stable. The standard enthalpy of formation determined by fluorine bomb technique at 298.15 K is $-(65.8 \pm 1.2)$ kcal mol^{-1} [39]. Estimation of the homogeneity range of MoS_2 was carried out in Ref. [40] by stepwise annealing with H_2 and analyzing the gas phase. There is no evidence for a homogeneity range of MoS_2 which is free from stacking faults, i.e. this homogeneity range is smaller than 8×10^{-5} mol S per mol of MoS_2 at temperatures between 1173 and 1373 K.

MoS_2 has a structure built of close-packed layers of sulfur atoms stacked to create trigonal prismatic interstices occupied by molybdenum. Only relatively weak Van der Waals bonding exists between layers, which causes lubricant properties of MoS_2 similar to those of graphite. Crystalline varieties 2*H*, 3*R*, and 1*T* of MoS_2 were reported [41–43]. The first two differ by

layers' arrangement, whereas in the metastable 1*T* form the coordination of molybdenum atoms is distorted octahedral. According to Ref. [44] no surface reconstruction or relaxation occurs in the MoS_2 crystal. As follows from the structure, MoS_2 is a highly anisotropic layered material. Thus, electric conductivity parallel to the layer is 1000× greater than in the perpendicular direction [45].

The properties of the planes represented in Fig. 3 ensure the most important applications of MoS_2. The inert basal (00*l*) planes provide lubricity and photocatalytic properties, whereas (*h*00) and (0*k*0) edges are believed to accommodate catalytic centers in the MoS_2 based heterogeneous catalysts of hydrotreating. It is generally accepted by the catalytic community that the most active ''promoted'' hydrotreating Co(Ni)–MoS_2 catalysts contain Co or Ni atoms located at the edges of MoS_2 slabs (decoration model [46]). Correspondingly, the tasks of materials chemists developing these two types of materials are substantially different. Highly dispersed materials exposing many edges are desired for catalysis, whereas oxygen-free extended monolayers are preferred in tribology. Due to anisotropy, at least two parameters are important for describing any MoS_2 dispersion: the slabs' average length and their stacking.

The XRD patterns of MoS_2 are easy to interpret: in them the shape of the (002) peak reflects the state of layers' stacking, whereas the set of higher angle peaks may provide information about the crystallinity within the layers. Analysis on the peaks' broadness and their relative intensity might provide useful information about textural parameters prior to other more sophisticated characterizations.

MoS_2 is a semiconductor. The semiconducting gap in MoS_2 results from the ligand field splitting of the Mo 4d orbitals [47,48]. Due to the prismatic coordination of Mo atoms, degeneration is removed from t_{2g} orbitals. The electronic structure of MoS_2 has been calculated using either the band [49], or the ligand field [50] approaches. It can be considered that above the occupied sulfur p-bands there are occupied d_{z^2} and empty $d_{x^2-y^2}$, d_{xy}, d_{xz}, d_{yz} in the sequence followed from the ligand field splitting diagram. However, in many calculations a considerable mixing is detected between the levels d_{z^2} and ($d_{x^2-y^2}$, d_{xy}), with sulfur p-character orbitals [51].

MoS_2 shows optical spectra with indirect band gaps of 1.23 and 1.69 eV, respectively [52]. As a semiconductor it demonstrates the relationship between band gap and particle size. Optical spectra of quantum confined 4.5-nm size MoS_2 particles in the solution MoS_2 were studied in Ref. [53] and related to the details of zone structure. The absorption edge of the spectrum results from the direct transition between the Γ and K points in the Brillouin zone. The features below this edge were observed, due to the excitonic transitions. Though optical spectra of MoS_2 are strongly related to its morphology, there are quite few studies in the literature on them for the catalytic materials, for example supported systems. Further effort in this direction, namely a thorough comparative study of different model solids would be fruitful. The work [54] can be cited as an example, where the MoS_2 nanoclusters (S–Mo–S discs) were prepared with sizes 3.5-, 4.5- and 8-nm diameter. Their optical spectra were strongly different: 8-nm particles had a lowest absorption maximum at 473 nm, 4.5-nm particles had absorption maxima at 400 and 440 nm, and 3.5-nm size particles at 362 nm.

It is difficult to study the MoS_2 materials by the vibrational spectroscopies. MoS_2 is black and air-sensitive when highly dispersed. Therefore transmission IR studies of the unsupported MoS_2 pressed in pellets are hardly possible, but rather the diffusion reflectance under

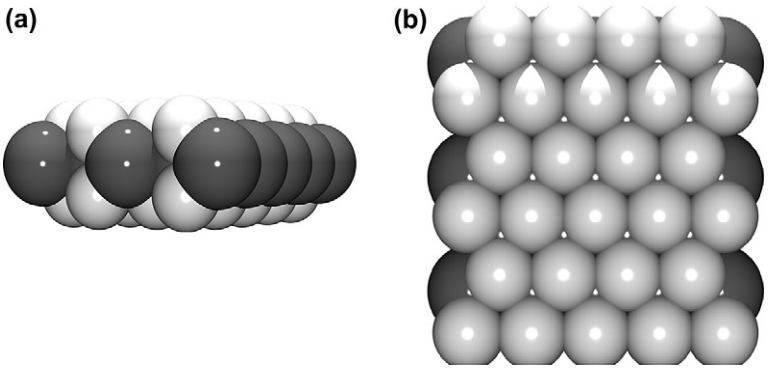

Fig 3. Van der Waals-scaled representation of a MoS_2 slab perpendicular to 100 (a) and 001 (b) axes of hexagonal MoS_2 structure. Box of enclosure 3 × 7 × 7 Å around a molybdenum atom was arbitrarily chosen. Light grey balls – sulfur; dark grey balls – molybdenum.

controlled atmosphere should be used. If studied in air by laser Raman spectroscopy, the samples of MoS_2 with high probability are burned by the laser beam, even at low beam power, and then they show only the MoO_3 spectrum. As the Mo–S bond has relatively low polarity, the IR extinction coefficients are low. However, Chang and Chan [55] succeeded to observe the IR and Raman spectra of MoS_2 (and amorphous MoS_3) using KBr and CsI pellets, which were rotated in the case of LRS measurements to avoid overheat. The IR bands at 385 and 470 cm^{-1} were observed for poorly crystalline MoS_2, while MoS_3 gave broad bands at 287, 335, 373 and 522 cm^{-1}. More recently Maugé et al. studied the infrared spectra of the unsupported MoS_2. Several features seen in the air-exposed samples are mostly due to the impurities, whereas the sulfide cleaned by heating in vacuum has virtually featureless spectrum (of course, besides the mentioned bands) [56].

The Raman signatures of single crystalline MoS_2 at 383 and 408 cm^{-1} correspond to the E^1_{2g}, and A^1_g modes of hexagonal MoS_2 respectively [57]. The band at 525–530 cm^{-1} often seen in the highly divided sulfide is due to the S–S vibrations of the edge-located disulfide groups.

Only a few core-level spectra of pure, well-defined MoS_2 have been published [58–60]. In the recent study [60] Matilla et al. thoroughly measured the Mo 3d and S 2p spectra using different excitation energies ranging from 200 to 350 eV for sulfur and from 280 to 400 eV for molybdenum. The fitted core level spectra of S 2p and Mo 3d states revealed several photon energy sensitive components. The S 2p spectra consisted of three and those of Mo 3d of four doublets. The high binding energy component in both spectra was supposed to originate from the uppermost sulfur or molybdenum atoms of an S–Mo–S sandwich layer of the hexagonal structure.

The MoS_2 slabs perpendicular to the (002) planes are easily observable by the transmission electron microscopy (TEM), whereas basal planes tend to escape from the observation, especially in the low-stacked solids. In the non-turbostatic specimens, rotation of the parallel slabs along the (00l) direction may lead to the moiré patterns (obviously of trigonal or hexagonal symmetry) which in some cases can be mistakenly interpreted as atomic structure images [61].

3. Preparation of MoS_2-based materials

As a majority of metal sulfides MoS_2 can be prepared by direct combination of the elements at high temperature crystalline MoS_2 powders have been prepared by the elemental reaction in vacuum at high-temperature [62] or by self-propagating high-temperature synthesis [63]. As follows from the DSC studies on reactions of the elements, molybdenum reacts with sulfur between 500 and 650 °C [64].

However, this review is devoted to the methods leading to some particular properties of the resulting materials. Many of them belong to the so-called soft chemistry (*chimie douce*) routes, where the preparation occurs at much lower temperatures than the corresponding solid-state reaction (note that still called conventional or traditional, the solid-state reactions are reported more and more rarely, being now much less studied than ''non-conventional'' ones, e.g. sol–gel or hydrothermal syntheses). The preparation techniques are divided into several groups. However, this division is sometimes arbitrary and subjective. The same preparation technique may belong to different groups. Thus sonochemical decomposition of aqueous thiomolybdate might be considered at once as precursor decomposition, solution reaction and sonochemical synthesis.

3.1. Sulfidation of the oxides

Probably the most studied technique of MoS_2 preparation is solid–gas sulfidation of the corresponding oxides. A bunch of work has been done on it since the procedures of sulfidation of supported oxides by mixtures of hydrogen sulfide and hydrogen are routinely used to activate hydrotreating catalysts. Formation of sulfide from the oxide requires reduction, since Mo(VI) species should be transformed to the Mo(IV) ones.

$$MoO_3 + 2H_2S + H_2 = MoS_2 + 3H_2O \quad (6)$$

However, molybdenum oxide species can be sulfided as well by pure hydrogen sulfide or its mixtures with any non-reacting gas. In this case hydrogen sulfide works at once as a sulfiding reducing agent, being necessarily decomposed to give some elementary sulfur:

$$MoO_3 + 3H_2S = MoS_2 + 3H_2O + 1/8S_8 \quad (7)$$

Finally, even the vapour of elemental sulfur at sufficiently high temperature suits to transform the oxide to MoS_2:

$$2MoO_3 + 7/8S_8 \rightarrow 2MoS_2 + 3SO_2 \quad (8)$$

Morphology control is not possible in such preparations because the reaction is topotactic and the MoO_3 dispersions are hardly available. Formation of thin film of MoS_2 and further reduction of MoO_3 by H_2S

occurs instead of sulfidation. Of course, MoO_3 can be used as a precursor in the (hydro)solvothermal syntheses and then the resulting process can be formally considered as oxides' sulfidation, as suggested by Qian and coworkers [65]. To prepare binary sulfides (WS_2, MoS_2, and V_5S_8) from the respective oxides, the powders of MoO_3 (WO_3, or V_2O_5), were reacted with $NH_3 \cdot H_2O$, and CS_2 in a stainless steel autoclave, which was sealed and kept at 500 °C for 10 h. Indeed, pure sulfides were obtained in this case. However, the oxides seem to be dissolved in basic solvothermal brine and final reaction of MoS_2 precipitation very probably occurs in the liquid phase, rather than by solid–liquid topotactic process. At least hydrated oxides such as $MoO_2(OH)_2$ become highly volatile under these conditions. Therefore such syntheses should be considered as hydrothermal ones. Note that flower-like morphology of MoS_2 observed in Ref. [65] is very similar to that obtained by hydrothermal preparations, as discussed below.

Stepwise mechanism of the bulk and supported molybdenum oxide sulfidation was extensively studied and debated, since it is a crucial step of the activation of industrially important hydrotreating catalysts [66–69]. Sulfidation of molybdenum oxide using $MoO_3/SiO_2/Si(100)$ model catalysts and Mo_3^{IV}–sulfur cluster compounds was studied in Ref. [70]. XPS spectra of the temperature-dependent sulfidation of $MoO_3/SiO_2/Si(100)$ model catalysts were compared with spectra of model compounds such as $(NH_4)_2[Mo_3S_{13}] \cdot H_2O$ and its thermal decomposition products. The spectra showed the presence of bridging disulfide ligands and Mo^V ions. The results of Ref. [70] suggested that the initial reaction of the MoO_3 precursor with H_2S/H_2 mixture occurs in two steps, including an O–S exchange followed by a Mo–S redox process. In Ref. [71] the sulfidation of crystalline MoO_3 and the thermal decomposition of $(NH_4)_2MoO_2S_2$ to MoS_2 have been studied by means of XPS and infrared emission spectroscopy (IRES). Basic steps of the sulfidation were proposed. The sulfidation reaction by means of reaction with H_2S starts already at low temperatures from an exchange of terminal O^{2-} species of MoO_3 for S^{2-}. In subsequent Mo–S redox reactions, bridging S_2^{2-} ligands and Mo^{5+} centers are formed. Above 200 °C, reduction occurs, transforming the Mo^{5+} centers to Mo^{4+} of MoS_2. Comparison of MoO_3 sulfidation with the decomposition experiments of $(NH_4)_2MoO_2S_2$ suggested that terminal O^{2-} ligands serve as the reactive sites (Fig. 4).

Many works deal with sulfidation of supported molybdenum oxide. Thus, the effects of surface orientation and crystallinity of alumina supports on the microstructures of molybdenum oxides and sulfides were addressed in Ref. [72]. Sulfidation of nickel- and cobalt-promoted molybdenum–alumina catalysts using a radioisotope ^{35}S-labeled H_2S pulse tracer method was studied in Ref. [73]. The sulfidation of supported

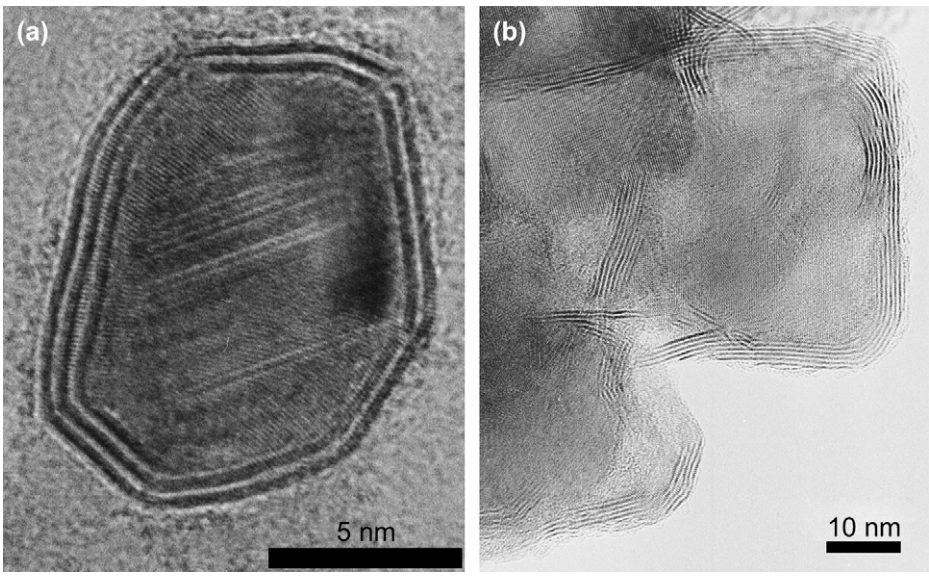

Fig. 4. (a) A particle of MoO_2, covered with MoS_2 slabs, obtained from the sulfidation of dispersed MoO_3 at 400 °C. Further advancement of the sulfidation would require higher temperatures. (b) An unsuccessfully prepared supported MoS_2/Al_2O_3 catalyst. Due to the presence of bulky oxide particles, the sulfidation is not complete and the catalytic activity of such a system is low (PA, 1994–1996, unpublished work).

(cobalt)molybdenum oxide catalysts was monitored by EXAFS [74–76]. Analysis of the oxidic catalysts showed that on the supported systems such as Mo/Al_2O_3 or Mo/TiO_2 the molybdenum oxide particles possess a highly distorted octahedral coordination of Mo with Mo–O distances ranging from 1.7 to 2 Å, which differ from one support to another and depend also on the preparation conditions. Upon sulfidation of the oxidic catalysts, small MoS_2 particles are formed and a Mo–Mo distance at 3.16 Å appears, characteristic of the MoS_2 structure. The activity of these catalysts can be controlled by optimizing the molybdenum sulfide–support interaction.

The above-cited works are just several examples and detailed discussion of supported MoS_2 systems is out of the scope of this review. The influence of support on the properties of MoS_2 catalysts was reviewed recently in Ref. [77].

In summary, sulfidation of solid oxide precursors is eminently important for the preparation of supported heterogeneous catalysts. However, this method is less convenient for the preparation of the unsupported MoS_2-based materials, if the applications at stake require finely dispersed materials.

3.2. Intercalation, exfoliation and restacking

Being a lamellar compound with the slabs connected only by Van der Waals interactions, MoS_2 may adopt various guest species between the layers. However, MoS_2 avoids direct intercalation, except for lithium. Passing through the lithium intercalates, diverse species can be intercalated such as naphthalene [78], amines [79], polymers [80,81] and so on. The intercalation chemistry of MoS_2 has been recently reviewed [82].

The general exfoliation and restacking scheme implies first the interaction of MoS_2 with butyllithium, leading to the intercalation of lithium (Li^0) between the sulfide slabs (step I, Fig. 5). Then the intercalated material is put into contact with water; lithium is oxidized, hydrogen is produced and the sulfide slabs are exfoliated, becoming monolayers dispersed in water (step II). Finally some coagulating (restacking) agent X is added and the slabs come back together, but now they contain X and one obtains a new material of restacked sulfide (step III). In a different approach of preparing alkali metal intercalated MoS_2, Li is replaced by the K cation. In this synthesis strategy the corresponding (hydrated) K_xMoS_2 phase might be prepared from the direct sulfidation of K_2MoS_4 thiomolybdate [83].

Different species may play the role of coagulant X. Up to now, a variety of MoS_2 based intercalated

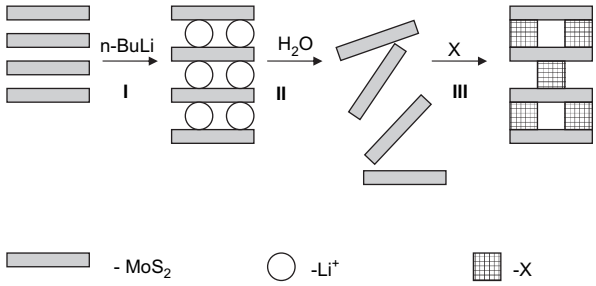

Fig. 5. General principle of the exfoliation–restacking technique.

materials including simple organic (trichloroethylene, styrene, phenanthroline, alkylammonium cations, etc.), polymeric, organometallic (metallocenes, ruthenium hydroxoarene complexes, etc.), and inorganic (post-transition metals, metal hydroxides) species have been prepared and characterized. Details on preparation and characterization of intercalates with different guests can be found in Refs. [84] (transition metal hydroxides), [85] (tetraalkylammonium cations), [86] (ruthenium hydroxoarene complexes), [87] (phenanthroline/phenanthrolinium). A surfactant molecule may stay for the X as well. In this case highly conducting Langmuir Blodgget films could be obtained [88].

The intercalation of lithium into MoS_2 [89,90] leads to a change in the electronic structure of the host layers due to a nearly complete one-electron transfer from Li to MoS_2 layers. This transfer leads to a change of Mo coordination from trigonal prismatic to octahedral and to the clustering of Mo atoms due to displacements from their ideal positions in the layer.

In the reaction of $LiMoS_2$ with water, lithium atoms pass into the solution as hydrated Li^+ ions, and partially negatively charged single layers of MoS_2 are formed. These layers slowly discharge in the dispersion due to a reaction with water, which produces molecular hydrogen and OH^- anions. Owing to a residual negative charge on the MoS_2 layers, the structural changes typical of $LiMoS_2$ are partially retained in MoS_2 single-layer dispersions and in some solid intercalated materials freshly prepared from them [91,92].

Upon intercalation, the local coordination geometry of the Mo centers of the host lattice changes from trigonal prismatic to distorted octahedral (as in the metastable 1*T*-MoS_2). This 2*H* to 1*T* phase transition is accompanied by considerable changes in the band structure, an increased electron density on the sulfur atoms of the MoS_2 lattice, and the formation of different types of superstructures [93,94].

While restacked MoS_2 is prepared from lithium intercalates, 1*T*-MoS_2 was prepared from K_2MoO_4 by sulfidation, subsequent reduction, hydration and

oxidation [83]. Their comparison was useful to sort out some confusion about the chemical and structural identity of restacked MoS_2 and WS_2. In 1999, the topic was revisited by Heising and Kanatzidis [95,96]. They questioned: are the layers of restacked MoS_2 neutral or charged, and why do 1*T*-MoS_2 and restacked MoS_2 have different superlattices? Indeed, restacked MoS_2 can incorporate both cationic and neutral species. Another point was: why restacked MoS_2 and WS_2 are p-type metallic conductors? The problem to answer if the layers are charged was that both negative and positive ions, Li^+ and OH^-, are present during the exfoliation. The lithium cation can counterbalance a negative charge on the layers when neutral species are intercalated, which is a difficult element to detect. The OH^-, which could co-intercalate with the cationic species, can be confused with residual water.

To sort out these points, the authors studied the relationship between charge and structure in restacked MoS_2 (and WS_2) by elemental analysis, electron diffraction, X-ray diffraction, and differential scanning calorimetry. Alkali cations have been encapsulated in MoS_2 and WS_2 without the presence of a co-intercalated counterion, suggesting a negative charge in the 0.15–0.25 electrons per M atom range. Electron diffraction studies showed ordering of these cations between the layers. Structure of restacked MoS_2 and WS_2 was elucidated by electron crystallography. It has been concluded that the seemingly trigonal structure is in fact an overlap of three individual orthorhombic crystals. Using two-dimensional *hk*0 data from films for both ''triple'' and ''single'' crystals, the authors showed that a severe distortion exists in the Mo/W plane, forming infinite zigzag chains. Therefore, they concluded that restacked MoS_2 and WS_2 are not 1*T* form but rather WTe_2 type.

The main interest of this method is to make new materials by intercalating some species between the MoS_2 layers. As with sulfide itself, freshly prepared from single-layer dispersions, MoS_2 exhibits substantial changes of the Mo atom cationic surrounding, as compared to the parent 2*H*-MoS_2. However, in general, unless they are occasionally cracked or strongly deformed by the chemical reaction, the resulting 2*H*-MoS_2 layers should more or less preserve their identity after exfoliation–restacking, when they relaxed back to the trigonal prismatic coordination. Therefore what we finally can expect from this method is to change the stacking mode and extent of MoS_2 layers, for example from turbostatic to non-turbostatic. This can be a drawback if one has a goal of preparing highly active catalysts. Indeed if we continue to believe that the catalytic activity is mostly due to the edges of the MoS_2 slabs, then the exfoliation–restacking should not give any great gain of catalytic activity because it does not change the edges amount. Therefore, in order to have a good catalyst, short slabs with important amount of edges should be prepared by some other technique and then they might be only altered by exfoliation–restacking, for example by being intercalated with cobalt. Depending on the view point, this drawback can become an advantage. If the goal is a fine control of the material properties, then exfoliation–restacking is a good technique since it allows (at least in theory) to change only one parameter of stacking, leaving that of slab's length unchanged.

3.3. Decomposition of precursors

Obtaining MoS_2 by decomposition of some precursor implies that the sulfur necessary for the formation of the target phase is already present inside the decomposing solid and not brought in it by any exterior sulfiding agent (gas, liquid). On the other hand, the precursor is decomposed directly to give MoS_2 and is not pre-dissolved in any reaction medium (in which case we will speak about solution reactions). Therefore topochemical decomposition reactions of solids are under consideration here.

Probably the first preparation of MoS_2 by decomposition of molecular precursor $(NH_4)_2MoS_4$ was done by Bertzelius [97]. Somewhat later, high-surface-area MoS_2 was prepared by decomposition of a MoS_3 precursor by Eggertsen and Roberts [98]. Rapid conversion from trisulfide to disulfide at 723 K by sudden introduction of the MoS_3 sample into the hot zone yielded an unusually high surface area of 158 m^2/g, whereas slow decomposition (heating rate 20 K per min) produced much lower surface areas. Closer inspection of this work's results leads to the conclusion that the surface areas changed rather irregularly and the important parameter was rather the MoS_3 conditioning, but the fact of high-surface-area MoS_2 preparation is sure.

In recent years, many works have been carried out on the decomposition of thiomolydbates or other sulfur-containing coordination compounds of molybdenum. The simplest molecular precursors are ammonium thiomolybdates. Many thiomolybdates were prepared and structurally characterized [99,100]. All of them give MoS_2 as an ultimate decomposition product.

The thermal decomposition of thiomolybdate $(NH_4)_2MoS_4$ was described earlier by Brito et al. [101] and occurs according to the above-mentioned reactions (2,3). The intermediate formed trisulfide has been reported to be stable till about 673 K; at higher temperature it decomposes to elemental sulfur and MoS_2. The

solids obtained from thiomolybdate decomposition at 400 °C in H_2S/H_2 flow possess specific surface areas of ca 50–60 m^2/g. Due to good reproducibility of properties, they can be used as a reference for unsupported MoS_2 catalysts to compare with other, more sophisticated preparations [102]. A typical thiomolybdate decomposition product is constituted by stacks of 4–7 slabs having 5–8-nm length, as exemplified in Fig. 6.

Walton et al. carried out the in situ study of ammonium thiomolybdate decomposition [103], using powder X-ray diffraction and MoK edge EXAFS. Isothermal decomposition at 120 °C led to MoS_3 which was stable at this temperature. No intermediates were detected between $(NH_4)_2MoS_4$ and MoS_3, in agreement with earlier studies.

By analogy with the decomposition of monomeric salt, similar stepwise decomposition route can be supposed for thiodimolybdate [104]:

$$(NH_4)_2Mo_2S_{12}\cdot 2H_2O \rightarrow Mo_2S_{11} + 2NH_3 + H_2S + 2H_2O \quad (9)$$

$$Mo_2S_{11} \rightarrow 2MoS_2 + 7/8S_8 \quad (10)$$

Alternatively, when the decomposition was carried out under hydrogen, the last reaction might be partially or totally replaced with the reaction (11), which has the same expected mass loss as the reaction (12).

$$Mo_2S_{11} + 7H_2 \rightarrow 2MoS_2 + 7H_2S \quad (11)$$

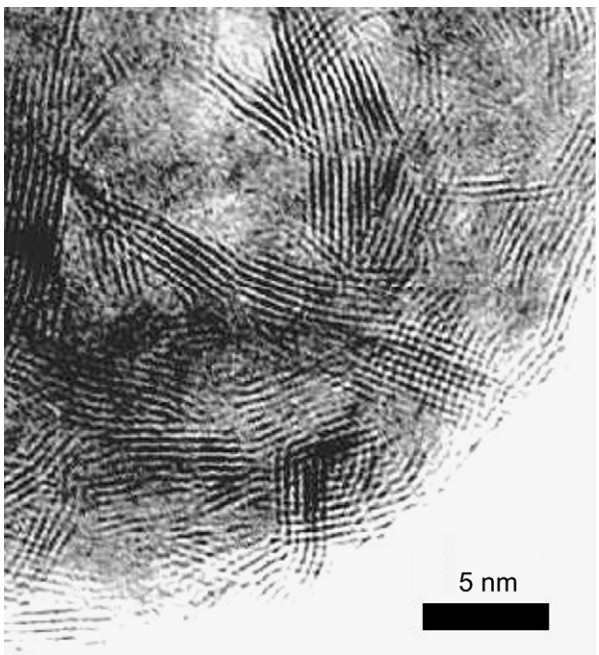

Fig. 6. MoS_2 slabs morphology for the product of decomposition of ammonium thiomolybdate at 400 °C in H_2S/H_2 flow (PA, 1999, unpublished work).

Thermal analysis and mass spectrometry results [104] corroborate these equations. The TDM salt decomposed to give amorphous molybdenum sulfide ($MoS_{5.5}$) as the intermediate product with simultaneous emission of NH_3 and H_2S. The amorphous nature of the $MoS_{5.5}$ solid follows from the X-ray powder pattern. Textural properties of MoS_2 obtained from the $(NH_4)_2Mo_2S_{12}$ decomposition are better (70–80 m^2/g, mesoporosity in the 2–8-nm range) compared to the products of monomeric thiomolybdate decomposition.

Earlier, the decomposition of thiomolybdates such as those including $(NH_4)_2Mo_3S_{13}$ to crystalline 2*H*-MoS_2 has been studied extensively by Müller et al. [105–108]. Topochemical relationship was supposed between the trinuclear cluster in the thiomolybdate and the disposition of Mo and S atoms in the resulting 2*H*-MoS_2.

Leist et al. showed that different ammonium thiomolybdates could be decomposed by heating in sealed quartz tubes, and in dynamic vacuum to 673 K, yielding onion-like MoS_2 with open edges [109]. It was noted that the precursor $(NH_4)_2Mo_3S_{13}\cdot H_2O$ shows decomposition behavior that is distinct from that of other ammonium thiomolybdates, in that its conversion to MoS_2 is characterized by a sharp exothermal event. The explanation provided was the topochemical nature of the reaction resulting from the structural relations between precursor and product. The HRTEM images in this work showed bent layers and the authors claimed their observation to be novel, so being them resembling the fullerene-like materials, however, not closed, but with the opened pores. It is worth noting that bent layers are very common in the dispersed MoS_2 materials and that the contrary is rather rare. However, this encouraged the authors to investigate the textural properties of their X-ray amorphous MoS_2 as obtained. The measurements of surface area, the pore diameter and volume showed that thermal decomposition of $(NH_4)_2Mo_3S_{13}\cdot H_2O$ resulted in materials with advantageous textural properties. Both the heat treatment and the presence of vacuum were necessary for porous materials to be obtained. The authors suggest that the driving out of volatile materials from the precursor and the ability of the MoS_2 slabs to form curved surfaces lead to the morphologies with large pores. Yet stability issues were not addressed in Ref. [109].

Worth emphasizing that the decomposition conditions play a crucial role on the materials' properties,

probably more important that the exact nature of the thiomolybdates used. Thus, our (unpublished) experience with trimolybdate was quite negative: we obtained molybdenum sulfide with specific surface area of only several square meters per gram. In that case we used large hydrothermally obtained $(NH_4)_2Mo_3S_{13}\cdot H_2O$ crystals and activated them at 673 K by the H_2S/H_2 mixture. It shows how different the conclusions may be if the authors do not use the same decomposition procedures.

Besides all-sulfur thiomolybdates, the salts of partially oxygen-substituted $MoOS_3^{2-}$ $MoOS_2^{2-}$ and MoO_3S^{2-} ions are known and relatively easily available. Their decomposition may also be used to produce highly dispersed MoS_2 materials and active Co–Mo–S heterogeneous catalysts [110].

In the last years, a number of works appeared on the preparation of dispersed molybdenum sulfide catalysts, using thermal decomposition of molecular precursors containing some organic part or doped by some extraneous organic species [111–113]. It appears that if the molybdenum sulfide contains at least several percent of carbonaceous matter, its textural (and catalytic) properties are greatly improved. Chianelli [114] was the first to point at the stabilizing role of carbon for the properties of sulfide catalysts. Since then, much research has been done on the topic and the positive role of a carbonaceous species was confirmed. These species can be contained in the precursor such as molybdenum naphthenate [111] or in the sulfidizing agents like DMDS. They might be introduced in the form as well of oxygenated organic admixtures [115,116] as of templating surfactants, either ionic or non-ionic [104]. Whatever the introduction way, the mechanism of their action seems to be similar.

Tetraalkylammonium thiomolybdate decomposition was extensively studied by Alonso, Chianelli and collaborators. The catalytic properties of MoS_2 and WS_2 catalysts obtained from the organics-containing thiosalts decomposition were found to depend strongly on the processing atmosphere, and heating conditions [117]. Large variations in surface area have been observed, from a few to several hundred square meters per gram [118,119]. Decomposition of tetraalkylammonium thiometallates $(NR_4)_2MS_4$ (M = Mo or W) at 350 °C in a flowing gas mixture H_2S/H_2 yielded highly dispersed catalysts MoS_2 or WS_2 [120]. Thiosalt decomposition is interesting as a method for obtaining better textural properties [121].

In situ technique involves heating the catalyst precursor and the reaction mixture containing a reactant, for example dibenzothiophene, in a closed pressurized reactor. In this process the simultaneous catalyst synthesis and catalyst activity measurement occur. There are several reports [112,122,123] on in situ decomposition of ammonium thiosalt precursors into high-activity and high-surface-area unsupported MoS_2 and WS_2 catalysts.

Thus, recent work [124] reports the development of a new technique for synthesizing highly porous unsupported catalytic materials. An isostatic pressure was first applied to the catalyst precursor in an open flow, and then heat was applied. Under this condition, as the organic components gradually decomposed and left the material, the voids left behind are immediately filled by the gas (pressure medium) in flow. The result was a very porous material with uniform pore size distribution. As the synthesis pressure increased, both surface area and catalytic activity of the materials produced increased. The catalytic activity value increased by a factor of 2 when the pressure increased from 6.9 to 55.2 bar. When N_2 gas was used as pressure medium it resulted in highly porous materials but low activity. H_2 appeared to be the ideal gas for both pressure medium and reducing agent. Co-promoted MoS_2 catalysts synthesized at 96.5 bar and 573 K showed particularly high catalytic activity [124].

In the methods described in this section, formation of the solids occurs upon the eruption of gaseous decomposition products from the body of the precursor towards its surface. By this reason, very strong impact of the decomposition conditions was observed, such as heating rate and final temperature, gas nature, its pressure and its flow rate. It can be compared to making bread in a bakery: whether the bread will be soft or hard and will it be covered with a crust depends on the pate composition but not on how the furnace is operated. The analogy can be supported by Fig. 7, where the same precursor decomposed in different conditions is represented. The products have very different morphology and if the conditions are not appropriate, a thick crust is formed (Fig. 7b).

The analogy can be continued even further, saying that only some empirically adjusted receipts are available from the literature and not any quantitative theories which would allow predicting MoS_2 morphology from a given set of precursor composition and decomposition conditions. Elegant as such, these methods often leave out of scope the questions of the thiomolybdate precursor preparation. Unfortunately, the latter might be laborious and industrially unfeasible. All literature techniques on the preparation of thiomolybdates include toxic and expensive ammonium sulfide or even worse, they require H_2S bubbling through the liquid reaction mixture. From the applied point of view, this might be the main drawback of such preparations, as any others which use thiomolybdates. The solution may come from the

optimization of the precursor preparations making them more user-friendly.

3.4. High temperature syntheses of MoS_2 nanotubes and fullerenes.

The discovery of nanotubes of carbon and carbon fullerenes has attracted great attention in the last years because of various interesting properties associated with their small dimensions and high anisotropy, including quantum effects [125,126], potential use as efficient field emitters and exceptional mechanical strength [127]. Nanotubular shape of matter appeared to be a brand new concept. Several reviews were published on the subject in the latest years, see for example [128].

At the same time a revision of values occurred in chemistry, and particularly in materials science, putting a strong accent onto the quasi one-dimensional and closed shell hollow objects of any kind. They were revalorized in the fields where they were previously considered as undesirable or just as insignificant curiosities. Thus, those structural chemists who previously considered obtaining of holey crystals as failed tentatives to grow good-quality monocrystals could see them much more positively as ''microtubules''. The revisions of this kind can occur by scientific but also by social reasons [129]. Earlier examples of such revisions included renaming critical phenomena and non-linear instabilities to ''synergetics'' and ''catastrophes theory''. More recently, due to the advent of the ''nano'' science field, well-known colloids and catalysts become new and fashionable ''nanoparticles''.

For many years onion-like structures of MoS_2 and WS_2 were routinely observed by the researchers working with sulfide catalysts in the highly loaded supported and unsupported catalysts. Usually they were observed in the case of incomplete sulfidation of oxide particles. Such particles had an onion-like structure and possessed an irregular faceted shape (see Fig. 4 of this review). However, after the discovery of fullerenes a new glance was given at this type of objects, mostly due to the works of Tenne et al. [130–132].

Finding that curled-up dichalcogenide sheets can also form tube-like objects and fullerene-like nanoparticles demonstrated that synthesis of nanotubes made of atoms other than carbon may be possible; 15-nm-diameter tubes made of tungsten and molybdenum disulfide have been reported [133,134]. The ultralow friction and wear properties of MoS_2 fullerene-like particles [135] make inorganic fullerenes promising lubricant materials. Fullerenes and nanotubes of MoS_2 have been prepared using reaction of MoO_3 micron-scale particles with H_2S at 800–950 °C [136,137]. Under similar conditions MoS_2 wires and tubes have been prepared. Thus microtubes with diameters of several microns and single walled MoS_2 fullerene nanotubes were both synthesized by iodine vapor transport of MoS_2 powder in vacuum at 740 °C by Remskar et al.

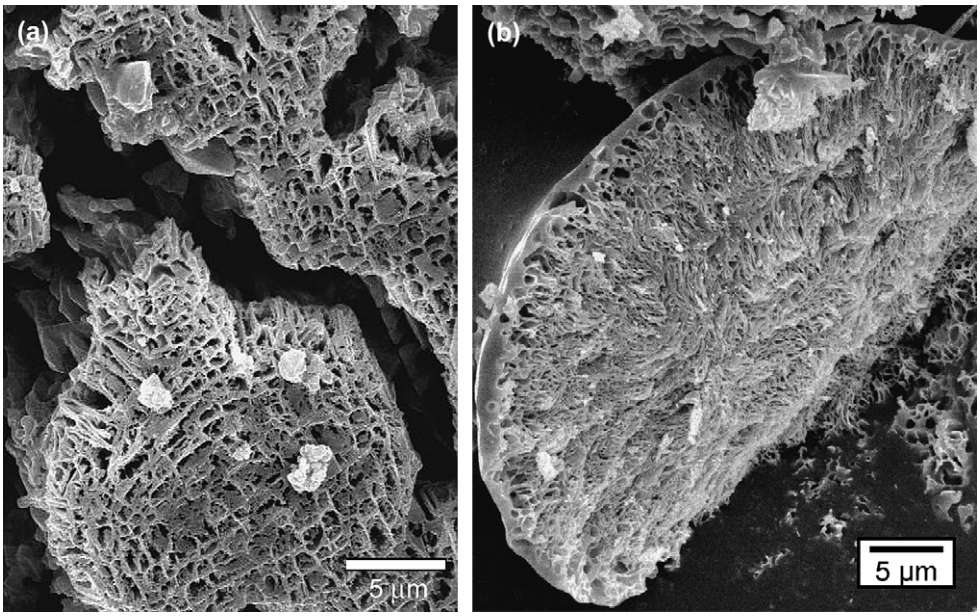

Fig. 7. Porous morphology of the MoS_2 obtained from decomposition of the precursors: (a) heating of the $(NR_4)_2MoOS_3$ (R = Et) at 400 °C, H_2S/H_2 flow, heating rate 10 min^{-1}; (b) heating of the same precursor at 400 °C, N_2 flow, heating rate 2 min^{-1} (PA, 2001).

[138,139]. Nanotubes with zigzag arrangements within the tube walls can be obtained by evaporation of MoS_2 at 1300 °C in H_2S [140].

While direct evidence was given of MoS_2 nanotubes preparation, it was not the case of fullerenes. In 1999 Parilla et al. [141] argued that the analogy of onion-like slabs reported by Tenne et al. to the carbon fullerene family falls short because no small preferred structure has been found. They obtained nano-octahedra of MoS_2 of discrete sizes in the soots prepared by laser ablation of pressed MoS_2 targets. These nano-octahedra had edge lengths of about 4.0 and 5.0 nm and according to the authors may represent the first true inorganic fullerenes. This point seems to be generally accepted now. Currently MoS_2 nano-octahedral are believed to be the smallest stable closed-cage structures of MoS_2, i.e., the genuine inorganic fullerenes. Structure and stability of such MoS_2 fullerenes was addressed recently in [142]. A combination of the experiments and density functional calculations with molecular dynamics annealing was used to elucidate the structures and electronic properties of octahedral MoS_2 fullerenes obtained by laser ablation. Targets of MoS_2 were laser-ablated and the soots analyzed by TEM. Multilayer nano-octahedra of MoS_2 were observed with 1000–25,000 atoms (Mo + S), in agreement with calculations.

As any hot research topic, fullerenes and nanotubes attract much effort and many disputable results are published. For example the fullerene-catalyzed and iodine-transported growth of ''MoS_2 nanotube bundles'' was reported in Ref. [143]. The reaction was carried out at 1010 K for 3 weeks in sealed tubes between MoS_2, iodine and fullerene. The resulting ''nanotube bundles'' contained 0.3 atoms of I per MoS_2 unit. The unit cell of the hexagonal close-packed ''bundles'' was reported to be 0.40 nm along the bundle axis and 0.96 nm perpendicular to the bundle, which are the dimensions characteristic for a compact molecular solid cell, not an assembly of (tightly packed as they could) individual solid objects. Moreover, according to the model proposed, the closest sulfur atoms of the adjacent ''nanotubes'' are separated by 0.35(1) nm, which corresponds to their Van der Waals diameters, whereas the distances within the ''tubes'' interior are even smaller and certainly correspond to the S–S binding. That means the ''nanotubes'', if any, are by no means hollow and their chemical identity is rather unclear, especially as concerns molybdenum coordination and its binding with iodine. Whatever they are, hardly one can consider these objects, as morphologically modified MoS_2. Note that using the logic of Ref. [143], many known and innocent chemical compounds containing in their structures chains or tunnels, may be reconsidered as the ''bundles of nanotubes''. On the other hand, due to attractiveness of this topic, in many papers the preparation of inorganic fullerenes or nanotubes was claimed without sufficient ground. Thus, for example the synthesis of nanocrystalline MoS_2 and WS_2 was described by Vollath and Szabó in Ref. [144]. The synthesis was performed by means of the reaction of the hexacarbonyls with H_2S in microwave plasma. The authors state that the particles exhibiting nested fullerene-like structures and polyhedron-shaped crystals were found. However, from the TEM images presented in the paper it follows that only a very small minority of MoS_2 slabs are similar to IF, if any.

As stated, this topic attracted considerable research effort and great number of the variations of the nanotubes and fullerenes' preparation techniques have been published since. Detailed discussion of all them is out of the scope of this review. The state of the field has been recently reviewed by Tenne [132]. Here note that all such preparations include only high-temperature treatment (800 °C or more) as long as the results seem reliable and correspond to some real nanotubes and/or fullerenes. From the catalysis point of view, it would be interesting to check whether the curved basal planes do demonstrate some modified properties. Indeed, unlike monoatomic thickness graphite plane, MoS_2 slab is triatomic. Therefore it is much more rigid and just cannot be curved without creating an important amount of defects breaking trigonal prismatic coordination of Mo atoms. In other words, a large part of Mo atoms should be in a modified environment, either by addition of an extra sulfur atom into the coordination shell or by creation of a vacancy. If the curvative is controlled by means of the nanotubes, size control, they might provide very interesting model systems for catalysis.

3.5. Hydrothermal and solventothermal preparations

Hydrothermal syntheses is a rapidly developing field nowadays. Probably the most important number of new compounds in solid-state chemistry is currently being prepared by this method. Naturally, sulfides' preparations were tried as well in these conditions, including MoS_2. Many recent papers report on such synthesis. In them, either the precursor already contains sulfur such as thiomolybdate and then simple hydrothermal decomposition might be sufficient, or it can be an oxide-state precursor. In the last case some sulfiding agent should be added (ammonium sulfide, thiourea, sulfur). Any general theory or even a predictive empirical approach for the preparations of this type is actually lacking,

therefore we deal more with the standalone preparation examples with varying synthesis parameters. Below we discuss some of them in order to analyze the possibilities of the method.

The hydrothermal synthesis allowed obtaining molybdenum sulfide with original morphology. Thus, in Ref. [145] we prepared MoS_2 by means of hydrothermal reactions of ammonium thiomolybdate. The reaction temperature and the acidity of the reaction mixture are key parameters, determining the nature of the products obtained. Varying these parameters, pure phases of needle-like $(NH_4)_2Mo_3S_{13}$ crystals or highly dispersed MoS_2 with very long layers have been prepared. They appeared to be interesting model solids to study the nature of catalytic function in the sulfide systems. Indeed, the length and stacking of the MoS_2 slabs are significantly different from those of samples obtained by thermal decomposition of the same precursor.

The surface areas of hydrothermal MoS_2 solids obtained in Ref. [145] were about 80–100 m^2/g, which is somewhat lower than those of carbon-stabilized samples. However, their stability was high, and being free of carbon, they were also free of its influence on the catalytic properties, whatever the last. Such a set of solids gives a good opportunity to study the structural sensitivity of the hydrogenation HYD and hydrodesulfurization (HDS) reactions. Indeed, there is still no agreement in the literature on the role of the sulfide morphology in the hydrotreating activity of MoS_2-based systems. The relative role of catalytic sites located at the rims and at the edges inside the MoS_2 stacks was supposed to be unequal in the HYD and HDS reaction, but because of the lack of appropriate model materials, no final solution was obtained for this problem. The detailed discussion of this complex problem is beyond the scope of this review and was treated in earlier reviews (e.g., Ref. [146]). In the work [145] we have seen that the HYD/HDS activity ratio was inverted in these experiments as a function of the catalyst morphology. Therefore control of Mo sulfide catalyst selectivity via the change of its morphology is indeed possible. Still the problem of rim-edge activity and the role of curved basal planes is unresolved.

Other recent examples of hydrothermal MoS_2 preparations can be found in the literature. Hydrothermal synthesis of MoS_2 and its pressure-related crystallization were studied by Peng et al. [147]. In this work ammonium molybdate $(NH_4)_6Mo_7O_{24}\cdot 4H_2O$, elemental sulfur, and hydrazine monohydrate reacted in an autoclave at 170–200 °C in the range of reaction times from 72 h to 30 days. The morphology was similar to that presented in Fig. 8. No specific surface area was reported.

Bokhimi et al. [148] studied thermal evolution in air and argon of nanocrystalline MoS_2 synthesized under hydrothermal conditions. Nanocrystalline molybdenum sulfide was synthesized between 150 and 225 °C under hydrothermal conditions starting from ammonium heptamolybdate and thiourea. Samples were characterized by X-ray powder diffraction, electron microscopy, nitrogen adsorption, thermal analysis and infrared spectroscopy. According to the authors, the initial MoS_2 crystals were bent and associated in bundles that formed worm-like grains interacting with each other to produce spherical grains aggregated in clusters. However, the specific surface area of the materials obtained were rather small (about 10 m^2/g). The morphology had again the flower-like aspect (the authors call it worm-like), which seems typical for the hydrothermal preparations.

In Ref. [149] hydrothermal synthesis of MoS_2 nanowires was reported. The authors claim to obtain the MoS_2 nanowires with diameters of 4 nm and lengths of 50 nm by a hydrothermal method using MoO_3 and Na_2S as precursors in a 4 mol/l HCl solution at 260 °C. The as-prepared MoS_2 had BET surface area of 107 m^2/g. The technique is simple, the precursors are convenient, and the properties of obtained MoS_2 advantageous. However, there seems to be no evidence of the announced nanowire structure (see discussion in Section 3.4). The solids look similar to other hydrothermal preparations and consist of long stacks of slabs which agglomerate to give flower-like (or worm-like) morphology as discussed above.

Simple solution route to uniform MoS_2 particles with randomly stacked layers was reported in Ref. [150]. MoS_2 particles of uniform size (ca. 70 nm) consisting of random and loosely stacked layers have been synthesized from hydrazine solution with $(NH_4)_2Mo_3S_{13}$ as the precursor at 180 °C for 16 h under hydrothermal conditions. The particles were characterized by X-ray diffraction (XRD), X-ray photoelectron spectroscopy (XPS) and high-resolution transmission electron microscopy (HREM). The influences of reaction conditions are discussed, while a mechanism is proposed to explain the formation of this peculiar morphology.

Tian et al. [151] report on synthesis of MoS_2 nanotubes and nanorods by hydrothermal technique at 180 °C. The preparation included reaction of MoO_3 with KSCN at 160, 180, 200 and 220 °C. The reaction mechanism was inferred from the analysis of the dried supernatant portion. The obtained MoS_2 had a morphology of micron-sized rods and tubes, with the walls

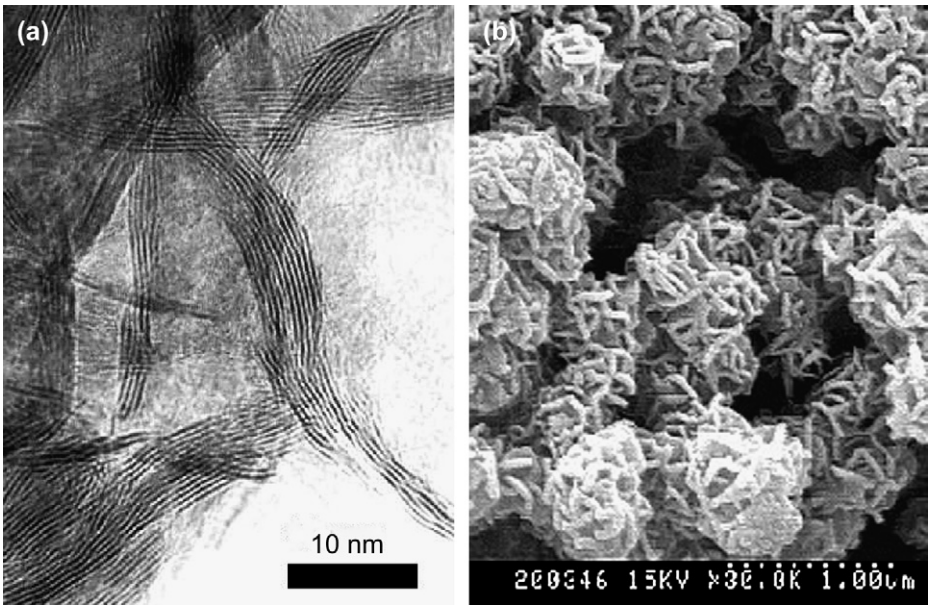

Fig 8. (a) TEM image of the MoS_2 layers obtained by hydrothermal decomposition of ammonium thiomolybdate (cf. Fig. 6). (b) SEM image of the same specimen. Preparation conditions are close to those described in Ref. [145].

constituted by typical ''hydrothermal MoS_2'' sheets. The large size of the rods and their complex morphology allow supposing that the reaction included dissolution of oxide and diffusion of the dissolved species (presumably molybdate MoO_4^{2-}), where they react to give sulfide. In any case, whatever the exact reaction mechanism, a MoO_3 can obviously be dissolved due to the basic pH of the thiocyanate solution.

Peng et al. prepared tube- and ball-like amorphous MoS_2 by a solvothermal method [152]. Reaction mixtures contained ammonium molybdate $[(NH_4)_6Mo_7O_{24}\cdot 4H_2O]$, elemental sulfur, lithium hydroxide monohydrate, $(NH_4)_2CO_3$ and hydrazine monohydrate. Pyridine was used as a solvent. The reaction temperature was 190 °C and duration 24 h. In this case obvious tubular and hollow spherical morphology was obtained, unlike the previously described preparations.

Analyzing this set of examples, we see that a variety of precursors and sulfiding agents can be used in this type of syntheses, in the range of temperatures approximately from 150 to 300 °C. The general tendency for the materials is to have an opened flower-like morphology, with the slab's length greater than that obtained by other techniques, probably due to advanced slabs growth under conditions allowing efficient mass transport. The stacking is not very high probably because the growing slabs are separated by the solvent molecules. The sheets have often ''rag-like'' shape similar to that reported by Chianelli et al. [153].

As a general criticism of this field as a whole it can be stated that often the papers reporting on the hydrothermal preparations just jump straightly to the materials without much care about chemical issues, trying neither to characterize them in depth nor to test their important properties for the applications. Often we do not know whether all the components added to the reaction mixture were necessary. The hydrothermal brines are used somewhat as a kind of magic hat from which this or that animal suddenly goes out. The materials as obtained are numerous and often seem to be interesting. However, in most cases only some general characterizations are presented as XRD and microscopy images. Better communication would be desirable between the inorganic chemists who are directly involved in the studies of (photo)catalytic or lubricant properties of the MoS_2-based materials. The hydrothermal preparations of MoS_2 are still waiting for their rationalization and systematic study, as concerns the mechanisms and the relations between the products' properties and the reaction conditions.

3.6. Solution reactions

In our classification solution syntheses are those in which no hydrothermal or solvothermal conditions are applied (i.e. no increased pressure of the solvent in the reaction mixture), but the target MoS_2 precipitates from a homogeneous solution. Very few works satisfy

this criterion. Less restrictively, the precipitate can be not only MoS_2 but also some sulfur-rich sulfide. The latter can be further transformed topotactically to MoS_2 by thermal decomposition. Slow solution reactions leading to amorphous precipitates seem to provide the best potential for the control of morphology. Indeed, in this case the precipitation is isotropic, similar to the TEOS hydrolysis in water (and we know how rich are the possibilities of morphological control in this latter case). Since amorphous isotropic particles are growing, no strong difference of energy between different morphologies should be expected. Therefore slight variations of parameters are sometimes sufficient to obtain strong variations of the precipitates' morphology, as illustrated below.

To produce MoS_2 directly in the aqueous solution, thiomolybdate precursor was applied [154–156]. Since the latter already contained sulfur, the treatment necessary was reduction with some strong enough and easy-to-remove agent, which was hydrazine. $(NH_4)_2MoS_4$ (ATM) was dissolved in water and reacted with the desired amount of $N_2H_4 \cdot H_2O$ with an ammonia or a HCl solution (for adjusting pH).

Formation of MoS_2 was possible in the pH range 7–10. Too low a pH leads to precipitation of amorphous MoS_3 according to the reaction. On the other hand, the samples prepared at too high a pH contain some impurities of MoO_2 (seen in the XRD pattern of the samples heated in nitrogen to 773 K). This fact can be explained by progressive hydrolysis of ATM to oxomolybdate, which reacts further with hydrazine, giving MoO_2.

The reaction allowed obtaining very short and randomly oriented fringes of MoS_2. The surface area of the so-obtained sulfide was from 100 to 150 m^2/g, but the great part of the surface was due to edges as can be directly seen in Fig. 9. Therefore very high catalytic activity is available. The reaction may be conducted in the presence of any appropriate support slurry; then highly active supported hydrotreating catalysts may be obtained [155,156].

Precipitation of sulfur-rich sulfides from the mixed solvents with their further transformation to MoS_2 was studied in Refs. [36,157,158]. This series of works has been initiated by "nanotubes fever" and by our inability to explain the genesis of some tubular morphologies observed in the experiment. Indeed, in most cases the tubules are produced due to the well-understood physical mechanisms, such as the strain release in the incommensurate lamellar structures [159] or assembly of some organic surfactant, or more generally due to some templates for which tubular morphology is well understood [160]. However, several syntheses of inorganic tubules did not fit to any of the known categories. Among them are for example the amorphous phosphorous nitride [161] and molybdenum sulfide hollow tubes [152,157] for which the physical mechanism of the

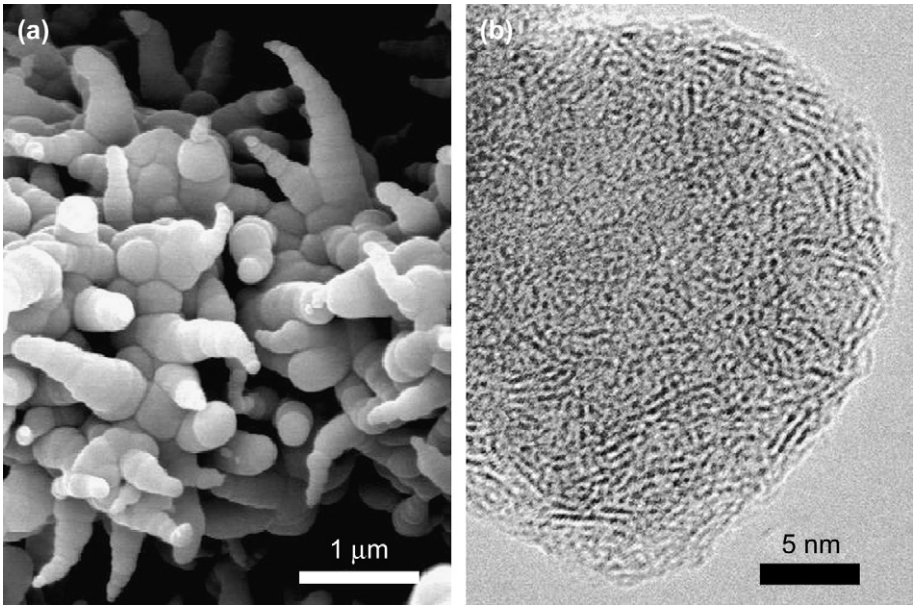

Fig. 9. (a) SEM morphology of MoS_2 obtained in aqueous solution at 90 °C from the thiomolybdate reduction by hydrazine. (b) TEM image of reduction of a spherical agglomerate in dried specimen. Weakly stacked and very short fringes are seen, but MoS_2 identity is not doubtful. The preparation conditions are similar to those of Ref. [154].

tubules and hollow sphere formation was unclear. However, despite the very different chemistry involved, the reported syntheses have some important similarity: the inorganic solids obtained are amorphous, whereas hollow or filled spheres and tubules coexist in them. As for the preparation conditions, they are carried out in the mixed solvents in the presence of dissolved electrolytes. The important point is that no external surfactant was added to the reaction mixtures to obtain such structures. These observations made us suggest that a general mechanism exists, leading to the amorphous hollow balls and tubules. The mechanism is supposed to be somewhat similar to that known for the micelles formation and vesiculation of lipids. In Ref. [158] we showed that the morphology of the amorphous MoS_x (and MoS_2 further obtained from it) might be controlled by the change of the ionic strength of the reaction mixture. Moreover, the types of morphologies similar to those known for the vesicles and tubular membranes are subsequently produced when the synthesis conditions are modified.

The morphology of the MoS_x precipitates was studied for the reaction of $(NH_4)_2Mo_2S_{12}$ (ammonium thiodimolybdate, ATDM) in water–acetone solutions in the presence of varying amounts of different electrolytes, such as NH_4SCN, KCl, $(NH_4)_2SO_4$ or $(NH_2OH_2)HSO_4$. To obtain vesicle-like and tubular structures, the content of the dissolved electrolyte should lie in the appropriate range, depending on its exact chemical composition. The electrolyte amount was found to be the key parameter, controlling the morphology obtained.

At low electrolyte content, microspheres were dominating (Fig. 10a). However, already at 1% concentration of the electrolyte added, the precipitate morphology is strongly changed. The surface of precipitate is not anymore smooth but covered with holes of different size. At the same time, at low electrolyte content, large vesicle like hollow spherical objects are sometimes observed. Further increase of the electrolyte concentration leads to production of tubular particles. The tubules are bent and heterogeneous in size, their diameter spans from tens to several hundreds of nanometers (Fig. 10b). Such a polydispersity is typical of the tubular vesicles of lipids [162]. The broad size distribution of the objects (tubes in the figure) suggests that the free energy of these metastable structures corresponds to flat and ill-defined minima in the variables' space (composition–temperature–ionic force). Heterogeneity of size and variable abundance of the structures also suggest that the difference in the formation energy of such objects is comparable to kT.

The effects observed are electrolyte non-specific, i.e. the same types of structures are produced while the electrolyte amount in the reaction mixture increases. Moreover, the electrolytes which are differently placed in the Hoffmeister series (strongly salting out $(NH_4)_2SO_4$, weakly salting out KCl, or salting in NH_4SCN), provided

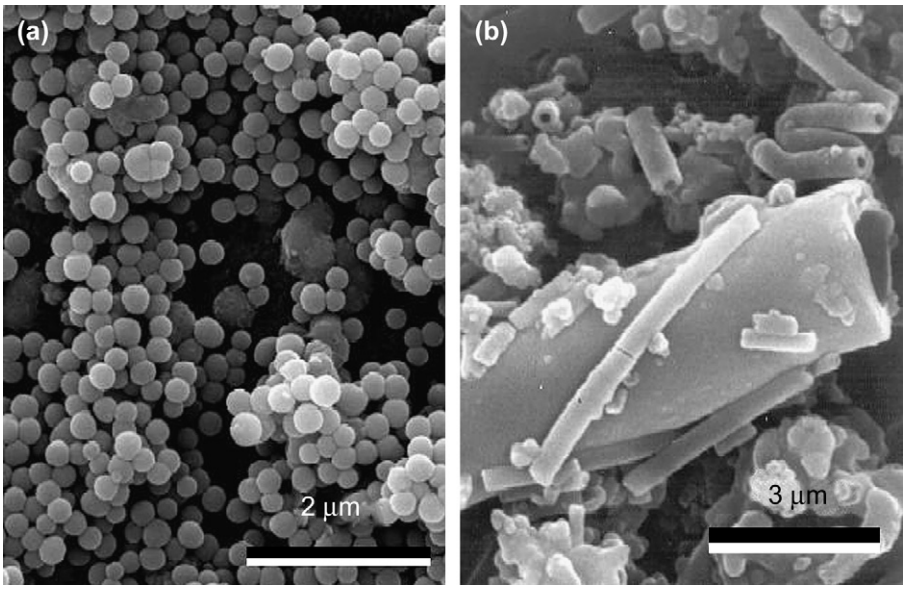

Fig. 10. (a) MoS_x microspheres obtained in the mixed acetone–water solution without electrolyte. Preparation conditions are close to those of Ref. [158]. (b) Heterogeneous-size MoS_x microtubules formed in the same solution in the presence of $(NH_4)_2SO_4$. There was no template or any surfactant added to the reaction mixture. Preparations are similar to those applied in Ref. [36].

the same effect. This behavior resembles strongly the behavior of the assemblies of amphiphilic molecules as a function of the packing parameter, while the system obeys the qualitative rules outlined by Israelachvili et al. for the organic micelles [163]. The variations of the ionic force are known to influence the size and the relative stability of the liposomes and vesicles [164,165]. Independently of the exact chemical structure of the species, the main idea was that carrying out a slow polymerization reaction in a mixed solvent in the presence of an electrolyte provides the possibility for growing oligomers to produce complex patterns. Imperatively, some short-range attraction and long-range repulsion forces must be present in a system for any space ordering to occur. In our case, the role of short-range attraction can be tentatively attributed to the interactions of the electrolyte ions with the ionic and polar Mo═O moieties of the growing oligomers, whereas selective structuring of water and acetone around the differently charged areas of the oligomers should correspond to the long-range repulsion. The common theoretical basis of description of such systems should present a natural extension of the existing approaches. Indeed, though the theories describing the formation of micelles and vesicles have been developed having in mind the organic amphiphilic molecules, the physical equations derived and the general rules of behavior following from them are indifferent to the exact chemical nature of the objects.

Low-temperature solution route to MoS_2 large fibers was reported by Liao et al. [166]. In this preparation, $(NH_4)_2Mo_3S_{13}$ was added to ethylenediamine at room temperature and stirred for 10 h. The black powder was collected and then annealed at 400 °C under N_2 atmosphere. It is not clear whether the MoS_2 was really obtained in the solution, since the properties of annealed solids are reported (and in this case MoS_2 should be formed anyways). Rather large size of the particles allows supposing that no dissolution of the precursor seemingly did occur in the reaction mixture but the process was topochemical reaction of thiomolybdate with liquid phase.

At last, the non-aqueous solution synthesis should be mentioned, where the controlled size single-layer MoS_2 disks were prepared as in Refs. [53,54]. This preparation used an inverse micelle where $MoCl_4$ was dissolved in ternary tridodecylmethylammonium iodide hexanol and octane, then reacted with H_2S or aqueous ammonium sulfide. The chemical reaction is obvious and includes exchange between chloride and sulfide anions through the micelle walls. Such preparations, though hard to imagine at a large scale, provide a fine size control of nanoclusters. An intriguing finding was made in Ref. [54] that the clusters of sizes 3.5, 4.5 and 8 nm can be prepared from polydisperse clusters, i.e. they correspond to the minima of free energy.

Overall, it seems that the solution preparations at low temperatures have great potentiality. However, often only amorphous MoS_x or ill-defined products are obtained and not directly the target MoS_2. Their further heating is needed to obtain MoS_2 with well-established chemical identity. Provided the decomposition products keep the morphology of initial amorphous precipitate, solution reactions can represent a powerful technique of morphological control.

3.7. Surfactant-assisted preparations

The syntheses using surfactant addition to improve the properties of the MoS_2 product can all be alternatively classified as hydrothermal or solvothermal techniques, or solution syntheses. What is important and makes them a separate group is the role of surfactant and its evolution during the synthesis. The MCM-inspired preparations of non-siliceous solids, including phosphates, non-siliceous oxides or chalcogenides were extensively studied in the last years. However, relatively few papers dealt with VI group sulfides, probably because of the lack of slow solution reactions which could be conveniently modified by the surfactant introduction. The works can be divided into two groups: those where some mesophases were identified, having low-angle XRD reflections and those where mesophases were not observed (or even were not researched) but the surfactant was applied just as a scaffolding species, in order to improve the textural properties of the synthesized solids.

In our work [110,167] we targeted first of all the synthesis of highly active hydrotreating catalysts. Therefore the ordering of porous system of the resulting solids was only of secondary importance. In Ref. [167] the surfactant-assisted preparation was carried out using the same reduction reaction of thiomolybdate by hydrazine precursors as in Ref. [154]. The only difference was the addition of cetyl-trimethyl-ammonium bromide (CTAB) to the reaction mixture. As a result, nearly perfect monolayers of MoS_2 were obtained, and they were stable after activation at 400–500 °C in the mixture H_2S/H_2. These preparations had specific surface area up to 210 m^2/g, one of the highest ever obtained for this compound. No mesophase was observed in the dried materials and we suppose that the surfactant plays in this case essentially the role of a scaffold, either before or after thermal activation.

In Ref. [110] the reaction applied and the surfactant added were completely different, but the idea of using a surfactant as a textural promoter was the same. The reactions of Co(II) or Ni(II) salts with thiomolybdates were used to generate the amorphous precipitates (12,13). The precipitates were further activated by conventional H_2S/H_2 treatment at 400 °C. The reactions (12,13) appear to provide a good ratio between Mo and Co(Ni) in the precipitate, which is further transformed to an unsupported catalyst.

$$Co^{2+} + MoS_4^{2-} \rightarrow CoMoS_4 \quad (12)$$

$$Co^{2+} + Mo_2S_{12}^{2-} \rightarrow CoMo_2S_{12} \quad (13)$$

The key point for obtaining highly dispersed catalysts using these reactions was the proper choice of the solvent and the organic admixture playing a role of textural promoter. Indeed, without the surfactant the aqueous reaction of thiomolybdates with Co(II) or Ni(II) salt solutions led to the immediate formation of black precipitates, but their further sulfidation produced solids with quite low HDS activities. A real improvement was only achieved after the addition of a textural promoter, which is a non-ionic surfactant of the alkylaryl-polyethylenglycol family (substances commercially known as Tergitols or Tritons). Another necessary admixture to the reactions solutions was ethylene glycol (EG): without it the addition of non-ionic surfactant led only to a moderate improvement of catalytic properties. As an explanation we speculated that EG acts as a solubilizing agent whereas the surfactant acts as a scaffold.

The precipitates obtained from the mixed solvent–surfactant solutions had a smooth morphology (Fig. 11). Sulfidation transformed them to fine dispersions, which according to the XRD contained only a MoS_2 phase without any cobalt-containing crystalline phases. Rietveld refinement of the patterns gives the value of stacking for the (002) broad peak, in the same sequence as that of the specific surface area values. Transmission microscopy of the sulfided catalysts shows the presence of short MoS_2 fringes as a unique component of the solid. The EDS study revealed that the solids are highly homogeneous, keeping almost the same Co/Mo atomic ratio. These catalysts demonstrated exceptionally high HDS activity in the hydrodesulfurization of substituted dibenzothiophene molecules, five times higher than that of the commercial catalyst of Ref. [110].

In the work of Ref. [168] micelle-assisted fabrication of necklace-shaped assembly of inorganic fullerene-like molybdenum disulfide nanospheres was stated. The preparation included anionic surfactant. In a typical synthesis, Na_2MoO_4 was reacted with hydrazine monohydrate and CS_2 in the presence of 1-octanol and sodium laurylsulfonate (SDS) at 140 °C for 24 h. Closer inspection of the results of this work shows that the particles have a typical "hydrothermal MoS_2" morphology. The linear assemblies of agglomerates are present; the slabs of MoS_2 are bent, but no evidence of closed "fullerene-like" shells was obtained.

The second group of works includes those where the authors pursued the goal of obtaining mesophases which would give small-angle XRD signature. The problem in

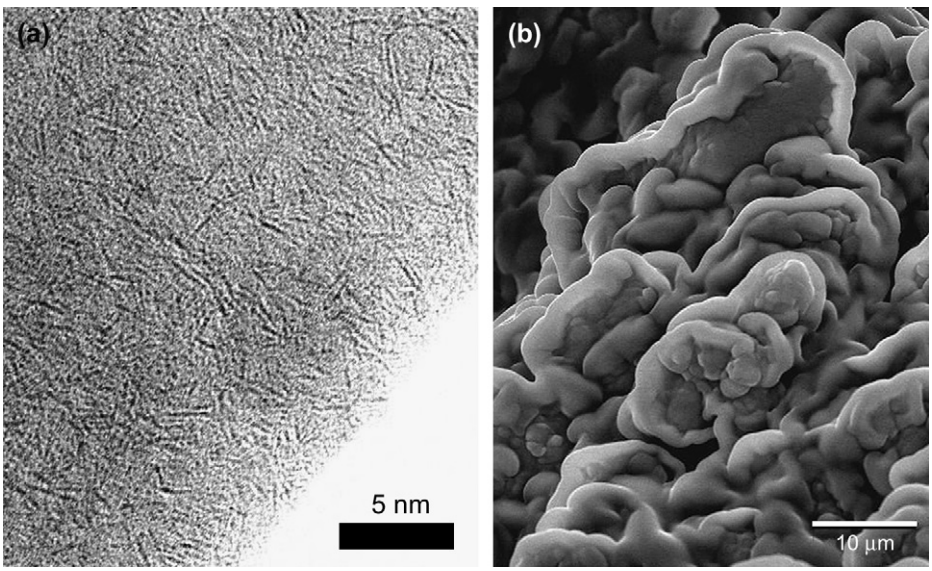

Fig. 11. (a) Monolayers of MoS_2 obtained from the reduction of thiomolybdate by hydrazine in the presence of CTAB [167]. (b) Morphology of the dried pre-catalyst from the precipitation of Co^{2+} with thiomolybdate in the presence of non-ionic Triton surfactant [110].

these studies was to preserve the ordering of pores after the removal of the surfactant. Mesolamellar molybdenum sulfides with intercalated cetyl-trimethyl-ammonium cations have been first prepared by Wang et al. at room temperature and under mild hydrothermal conditions [169]. In the hydrothermally treated sample, alternate dark and bright stripes are shown in the TEM images and the dark stripes were attributed to the inorganic molybdenum sulfide layers. However, the presented IR spectra suggest the formation of some partially hydrolysed oxoanions or amorphous MoS_3-like interlayer, but not of MoS_2. The two mesolamellar sulfide compounds are thermally unstable. The surfactant cations in the compounds start to decompose at about 200 °C with disappearance of the lamellar structure.

In Ref. [170] we obtained layered mesophases using the reaction between thiomolybdate and CTAB (14) and tried to transform it into mesolamellar MoS_2 hybride phase. Chemical composition and IR spectra of the products allowed supposing that an exchange reaction takes place:

$$2\mathrm{CTABr} + (\mathrm{NH_4})_2\mathrm{MoS_4} \rightarrow (\mathrm{CTA})_2\mathrm{MoS_4}\downarrow + 2\mathrm{NH_4Br} \qquad (14)$$

An XRD pattern of the layered structure was obtained with the three peaks observed in the low-angle region can be treated as (00l) series with maximum *d*-spacing equal to 30.5 Å. Further reduction of $(CTA)_2MoS_4$ by hydrazine was tried under mild conditions. Due to open structure of the starting material $(CTA)_2MoS_4$, hydrazine molecules could penetrate inside the inorganic layers and react further with $[MoS_4]^{2-}$. However, as a result of such treatment the interlayer thiomolybdates were transformed to dimeric oxothiomolybdates rather than reduced to MoS_2:

$$2[\mathrm{Mo^{VI}S_4}]^{2-} + 2\mathrm{H_2O} - 2\mathrm{e^-} \rightarrow [\mathrm{Mo_2^{V}O_2S_2(S_2)_2}]^{2-} + 2\mathrm{H_2S} \qquad (15)$$

At the same time the lamellar structure was preserved but the order of layers perturbed. Thermal decomposition of $(CTA)MoOS_{3.2}$ in argon flow led to formation of highly dispersed material having BET surface area 400 m^2/g. However, the layers' ordering completely disappeared due to the decomposition of the surfactant.

Recently, Kanadzidis and coworkers prepared Co–Mo–S mesophases [171]. The cobalt and nickel ions were combined with MoS_4^{2-} anions in the formamide solutions of the alkyl-pyridinium surfactant molecules CnPyBr, with *n* ranging from 12 to 20. The reaction mixtures were treated at 80 °C for several hours. Low-angle Bragg peaks in the range of distances 3.5–4.5 nm were observed in the XRD patterns of the products and lamellar mesostructure was put in evidence by TEM, in agreement with XRD. Unfortunately the mesostructure collapsed after heating above 673 K. Nevertheless the way of catalyst preparation through the Co(Ni)Mo–S mesophases seems to be interesting to pursue further.

Polycrystalline tubulenes and highly disordered sheets of MoS_2 were obtained in Ref. [172] by precipitating ammonium thiomolybdate solutions $[(NH_4)_2MoS_4]$ with two different tetraalkylammonium surfactants used as templates, hexadecyltrimethylammonium bromide $[CH_3(CH_2)_{15}N(CH_3)_3Br]$ and tetrabutylammonium hydroxide $[(CH_3(CH_2)_3)_4NOH]$. The surfactant-templated hybrid phase ($R_4N–MoS_4$) showed the (00l) diffraction peak series characteristic of a lamellar mesostructure. The hybrid phase was decomposed at temperatures above 600 °C, yielding a MoS_2 phase, which show unusual well-aligned bundles of tubulenes and sponge-like morphology.

As a summary, the surfactant-aided preparations showed their utility as concerns the improvement of textural properties of the materials obtained. However, no convincing evidence of obtaining MCM-like molybdenum sulfide was given as yet.

4. Conclusion

As can be seen from this review, for the preparation of highly dispersed MoS_2, a great variety of methods is now available. Within every technique further subdivision is possible, e.g. when talking about decomposition of molecular precursor, it can be static or dynamic; ex situ or in situ; the precursor can be thiocarbamate, thiomolybdate, thiocyanide and so on. Yet nothing has been said on such methods as electrochemical deposition of MoS_2 thin films [173–175] and CVD–MOCVD related techniques [176–181], molten salt [182,183] and sonochemical preparations [184–186].

Overall, MoS_2 is a readily available compound which is easily formed under various reaction conditions. Moreover it seems to be an ultimate product of almost any precursor decomposition and/or solution reaction at moderately high temperature if the active sulfide species and some reducing conditions are provided. That is probably why molybdenite is the naturally occurred mineral and the main source of molybdenum for industry. One can therefore easily propose yet other methods of MoS_2 synthesis. Thus, it can be expected that in the near future someone will come up with the microwave-assisted

preparations of MoS_2 or those using as a medium imidazolinium-type ionic liquids (or, better, both combined). However, for any new method of MoS_2 preparation to present some interest now, the important points are those of simplicity and/or the possibility to obtain MoS_2 with some original properties. The challenge is therefore not just to obtain MoS_2, but to obtain it simply, not expensively and with desired properties.

As a material and especially as a catalyst, MoS_2 still presents an interesting unresolved problem, concerning the relationship between its morphology, as seen by XRD and TEM, and its textural properties, as measured by gases' adsorption. That means, one may get a sample of MoS_2 showing some nice slabs of sulfide, both by length and by stacking resembling for example ex-thiomolybdate, but without any apparent reason having very low surface area according to nitrogen adsorption BET measurements. This fact is well known by the researchers working with MoS_2-based catalysts, but has never been explained (and never referenced). Indeed, for the unsupported MoS_2 catalysts after typical HDS catalytic tests (several days at 623 K, 0.1 MPa of hydrogen) the surface area drops usually by several times, e.g. from 60 to ca 15–20 m^2/g. At the same time no substantial change occurred according to XRD or TEM observations. This was not due to coking because the amount of carbon in the used catalyst was low. Some preparation techniques not including carbonaceous species also give this effect. Thus, this author observed a sample (obtained from the molybdenum nitride sulfidation) which had only 0.5 m^2/g specific surface area but which was virtually undistinguishable by XRD and TEM from the 60 m^2/g ex-thiomolybdate reference. This is very probably due to the fine details of the fringes packing. A study clarifying this problem could be interesting. To address this point, simultaneous TEM, BET and small-angle scattering (SAXS, INS) might be helpful.

The role of the bent basal planes remains an intriguing issue to understand. Though curved planes are omnipresent in the hydrotreating catalysts, the models existing now represent only flat hexagons (since recently, triangles) of MoS_2 and focus only on their edges. However, many findings contradict the simple edge decoration model of MoS_2 catalysts, see for example [120,187]. The questions therefore are: what is the coordination of molybdenum in the curved planes? Are the curved basal planes totally inactive? A systematic study taking advantage of currently available MoS_2 model solids with versatile morphology would be eminently relevant to sort out these points.

Finally, despite all the efforts made, the morphology control still remains a challenge. If many papers cited in this review claim that morphology control is achieved, no one really provides a technique of control, i.e. reproducible fine tuning of the MoS_2 properties by varying some synthesis parameters (unless we consider as such the decrease of surface area vs. sintering temperature, but this is rather a degenerate case). The only exceptions are probably the syntheses in the inverse micelles [54], but they are excessively complicated. What the earlier works provide is only (hopefully) the repeatability of properties or at best the qualitative change of morphology type as a function of preparation conditions. Applying different methods from the procedures published, qualitatively different MoS_2 specimens are now available, e.g. strongly stacked with short fringes or weakly stacked with long fringes, or monolayer MoS_2 slabs. However, what would be eminently interesting for catalysis and photochemistry is to be able to vary independently the fringes stacking and their length within one unique technique. Doing that within narrow range and getting specimens with stable stacking/length parameters would allow being more quantitative in the evaluation of different models of catalytic performance, as well as the quantum effects. To meet this challenge a technique should be developed in which the parameters of nucleation, growth and agglomeration of the MoS_2 slabs would be separately variable.

References

[1] T.G. Spiro (Ed.), Molybdenum Enzymes, Wiley, NY, 1985.
[2] S.P. Cramer, K.O. Hodgson, W.O. Gillum, L.E. Mortenson, J. Am. Chem. Soc. 100 (1978) 3398.
[3] S.P. Cramer, H.B. Gray, K.V. Rajagopalan, J. Am. Chem. Soc. 101 (1979) 2172.
[4] T.D. Tullius, D.M. Kurtz, S.D. Conradson, K.O. Hodgson, J. Am. Chem. Soc. 101 (1979) 2776.
[5] J. Bordas, R.C. Bray, C.D. Garner, S. Gutteridge, S.S. Hasnain, Biochem. J. 191 (1980) 499.
[6] E.I. Stiefel, Prog. Inorg. Chem. 22 (1977) 1.
[7] A.I. Hadjikyriacou, D. Coucouvanis, Inorg. Chem. 26 (1987) 2400.
[8] T. Shibahara, Coord. Chem. Rev. 123 (1993) 73.
[9] R. Chevrel, M. Sergent, J. Prigent, Mater. Res. Bull. 9 (1974) 1487.
[10] M. Potel, P. Gougeon, R. Chevrel, M. Sergent, Rev. Chim. Miner. 21 (1984) 509.
[11] S. Belin, R. Chevrel, M. Sergent, Mater. Res. Bull. 33 (1998) 43.
[12] M. Sergent, Ø. Fischer, M. Decroux, C. Perrin, R. Chevrel, J. Solid State Chem. 22 (1977) 87.
[13] E.P. Khlybov, G.M. Kuz'micheva, V.V. Evdokimova, Zh. Neorg. Khim. 31 (1986) 1102.
[14] W.J. Schutte, F. Disselborg, J.L. de Boer, Acta Crystallogr. B 49 (1993) 787.
[15] M.H. Rashid, D.J. Sellmyer, V. Katkanant, R.D. Kirby, Solid State Commun. 43 (1982) 675.
[16] J.M. Tarascon, G.W. Hull, Mater. Res. Bull. 21 (1986) 859.

[17] H. Yagoda, H.A. Fales, J. Am. Chem. Soc. 58 (1936) 1496.
[18] G. Laperriere, B. Matsan, D. Belanger, Synth. Met. 29 (1989) 201.
[19] T. Weber, J.C. Muijsers, J.W. Niemantsverdriet, J. Phys. Chem. 99 (1995) 9194.
[20] A.J. Jacobson, R.R. Chianelli, S.M. Rich, M.S. Whittingham, Mater. Res. Bull. 14 (1979) 1437.
[21] K.S. Liang, S.P. Cramer, A.J. Jacobson, C.H. Chang, J.P. de Neufville, R.R. Chianelli, F.J. Betts, J. Non-Cryst. Solids 42 (1980) 345.
[22] E.Z. Diemann, Z. Anorg. Allg. Chem. 432 (1977) 127.
[23] F.Z. Chien, S.C. Moss, K.S. Liang, R.R. Chianelli, Phys. Rev. B 29 (1984) 4606.
[24] S.P. Cramer, K.S. Liang, A.J. Jacobson, C.H. Chang, R.R. Chianelli, Inorg. Chem. 23 (1984) 1215.
[25] D.R. Huntley, T.G. Parham, R.P. Merril, M.J. Sienko, Inorg. Chem. 22 (1983) 4144.
[26] R.A. Scott, A.J. Jacobson, R.R. Chianelli, W.-H. Pan, E.I. Stiefel, K.O. Hodgson, S.P. Cramer, Inorg. Chem. 25 (1986) 1461.
[27] S.J. Hibble, D.A. Rice, D.M. Pickup, M.P. Beer, Inorg. Chem. 34 (1995) 5109.
[28] A. Müller, E. Diemann, E. Krickemeyer, H.J. Walberg, H. Bogge, A. Armatage, Eur. J. Solid State Inorg. Chem. 30 (1993) 565.
[29] K.S. Liang, J.P. de Neufville, A.J. Jacobson, R.R. Chianelli, F.J. Betts, J. Non-Cryst. Solids 35 (1980) 1249.
[30] S.J. Hibble, R.I. Walton, D.M. Pickup, A.C. Hannon, J. Non-Cryst. Solids 232–234 (1998) 434.
[31] J. Grimblot, Catal. Today 41 (1998) 111.
[32] R. Iwamoto, K. Inamura, T. Nozaki, A. Iino, Appl. Catal. A 163 (1997) 217.
[33] L. Busetto, A. Vaccari, G. Martini, J. Phys. Chem. 85 (1981) 1927.
[34] D.A. Rice, S.J. Hibble, M.J. Almond, K.A. Hassan Mohhamad, S.P. Pearse, J. Mater. Chem. 2 (1992) 895.
[35] G.F. Khudorozhko, L.G. Bulusheva, L.N. Mazalov, V.E. Fedorov, E.A. Kravtsova, I.P. Asanov, G.K. Parygina, Yu.V. Mironov, J. Morales, J. Phys. Chem. Solids 59 (1998) 283.
[36] P. Afanasiev, I. Bezverkhyy, Chem. Mater. 14 (2002) 2826.
[37] H. Topsøe, B.S. Clausen, F.E. Massoth, Hydrotreating Catalysis, Springer, Berlin, 1996, p. 1.
[38] L. Cizaire, B. Vacher, T. Le Mogne, J.M. Martin, L. Rapoport, A. Margolin, R. Tenne, Surf. Coat. Technol. 160 (2002) 282.
[39] P.A.G. O'Hare, E. Benn, F. Yu Cheng, G. Kuzmycz, J. Chem. Thermodyn. 2 (1970) 797.
[40] H. Rau, J. Phys. Chem. Solids 41 (1980) 765.
[41] R. Murray, B.L. Evans, J. Appl. Crystallogr. 12 (1979) 312.
[42] R.E. Bell, R.E. Herfert, J. Am. Chem. Soc. 79 (1957) 3351.
[43] F. Wypych, R. Schok llhorn, Chem. Commun. (1992) 1386.
[44] K.T. Park, M. Richards-Babb, J.S. Hess, J. Weissand, K. Klier, Phys. Rev. B 54 (1996) 5471.
[45] J.A. Wilson, A.D. Yoffe, Adv. Phys. 18 (1969) 193.
[46] H. Topsøe, B.S. Clausen, R. Candia, C. Wivel, S. Morup, J. Catal. 68 (1981) 433.
[47] R. Coehoorn, C. Haas, J. Dijikstra, C.J.F. Flipse, R.A. de Groot, A. Wold, Phys. Rev. B 35 (1987) 6195.
[48] R. Coehoorn, C. Haas, R.A. de Groot, Phys. Rev. B 35 (1987) 6203.
[49] L.F. Mattheiss, Phys. Rev. B 8 (1973) 3719.
[50] J.B. Goodenough, Phys. Rev. 171 (1968) 466.
[51] K.A. Yee, T. Hughbanks, Inorg. Chem. 30 (1991) 2321.
[52] K.K. Kam, B.A. Parkinson, J. Phys. Chem. 86 (1982) 463.
[53] J.P. Wilcoxon, G.A. Samara, Phys. Rev. B 51 (1995) 7299.
[54] V. Chikan, D.F. Kelley, J. Phys. Chem. 106 (2002) 3794.
[55] C.H. Chang, S.S. Chan, J. Catal. 72 (1981) 139.
[56] F. Maugé, J. Lamotte, N.S. Nesterenko, O. Manoilova, A.A. Tsyganenko, Catal. Today 70 (2001) 271.
[57] G.L. Frey, R. Tenne, Phys. Rev. B 60 (1999) 2883.
[58] M.A. Baker, R. Gilmore, C. Lenardi, W. Gissler, Appl. Surf. Sci. 150 (1999) 255.
[59] N.S. McIntyre, P.A. Spevack, G. Beamson, D. Briggs, Surf. Sci. Lett. 237 (1990) L390.
[60] S. Mattila, J.A. Leiro, M. Heinonen, T. Laiho, Surf. Sci. 600 (2006) 5168.
[61] J. Reyes-Gasga, S. Tehuacanero, M.J. Yacaman, Microsc. Res. Technol. 40 (1998) 2.
[62] R.N. Viswanath, S. Ramasmy, J. Mater. Sci. 25 (1990) 5029.
[63] P.R. Bonneau, R.F. Jarvis, R.B. Kaner, Nature 349 (1991) 510.
[64] H. Wada, K. Takada, T. Sasaki, Solid State Ionics 172 (2004) 421.
[65] X. Chen, X. Wang, Z. Wang, W. Yu, Y. Qian, Mater. Chem. Phys. 87 (2004) 327.
[66] C. Glasson, C. Geantet, M. Lacroix, F. Labruyère, P. Dufresne, Catal. Today 45 (1998) 341.
[67] V.H.J. de Beer, C. Bevelander, T.H.M. van Sint Field, P.G.A.J. Werter, C.H. Amberg, J. Catal. 43 (1976) 68.
[68] S.I. Kim, S.I. Woo, Appl. Catal. 78 (1991) 109.
[69] R.A. Prada-Silvy, P. Grange, B. Delmon, in: D.L. Trimm (Ed.), Catalysts in Petroleum Refining, Elsevier, Amsterdam, 1989, p. 233.
[70] J.C. Muijsers, T. Weber, R.M. Vanhardeveld, H.W. Zandbergen, J.W. Niemantsverdriet, J. Catal. 157 (1995) 698.
[71] T. Weber, J.C. Muijsers, J.H.M.C. van Wolput, C.P.J. Verhagen, J.W. Niemantsverdriet, J. Phys. Chem. 100 (1996) 14144.
[72] Y. Sakashita, Surf. Sci. 489 (2001) 45.
[73] W. Qian, A. Ishihara, Y. Aoyama, T. Kabe, Appl. Catal. A 196 (2000) 103.
[74] R.G. Leliveld, A.J. van Dillen, J.W. Geus, D.C. Koningsberger, J. Catal. 171 (1997) 115.
[75] R.G. Leliveld, A.J. van Dillen, J.W. Geus, D.C. Koningsberger, J. Catal. 165 (1997) 184.
[76] M. de Boer, A.J. van Dillen, D.C. Koningsberger, J.W. Geus, J. Phys. Chem. 98 (1994) 7862.
[77] M. Breysse, P. Afanasiev, C. Geantet, M. Vrinat, Catal. Today 86 (2003) 5.
[78] L. Kosidowski, A.W. Powell, Chem. Commun. (1998) 2201.
[79] V. Sanchez, E. Benavente, M.A. Santa Ana, G. Gonzalez, Chem. Mater. 11 (1999) 2296.
[80] M.G. Kanatzidis, R. Bissessur, D.C. De Groot, J.L. Schindler, C.R. Kannewurf, Chem. Mater. 5 (1993) 595.
[81] R. Bissessur, M.G. Kanatzidis, J.L. Schindler, C.R. Kannewurf, Chem. Commun. (1993) 1582.
[82] E. Benavente, M.A. Santa Ana, F. Mendizabal, G. Gonzalez, Coord. Chem. Rev. 224 (2002) 87.
[83] F. Wypych, K. Sollmann, R. Schöllhorn, Mater. Res. Bull. 27 (1992) 545.
[84] A.S. Golub, G.A. Protzenko, I.M. Yanovskaya, O.L. Lependina, Yu.N. Novikov, Mendeleev Commun. (1993) 199.
[85] A.S. Golub, G.A. Protzenko, L.V. Gumileva, A.G. Buyanovskaya, Yu.N. Novikov, Izv. Akad. Nauk, Ser. Khim. 4 (1993) 672.
[86] A.S. Golub, I.B. Shumilova, Yu.V. Zubavichus, M. Jahncke, G. Süss-Fink, M. Danot, Yu.N. Novikov, J. Mater. Chem. 7 (1997) 163.
[87] A.S. Golub, I.B. Shumilova, Yu.N. Novikov, J.L. Mansot, M. Danot, Solid State Ionics 91 (1996) 307.

[88] H. Tachibana, Y. Yamanaka, H. Sakai, M. Abe, M. Matsumoto, Chem. Mater. 12 (2000) 854.
[89] M.A. Py, R.R. Haering, Can. J. Phys. 61 (1983) 76.
[90] K. Chrissafis, M. Zamani, K. Kambas, J. Stoemenos, N.A. Economou, Mater. Sci. Eng., B 3 (1989) 145.
[91] P. Joensen, E.D. Crozier, N. Alberding, R.F. Frindt, J. Phys. Chem. 20 (1987) 4043.
[92] Yu.V. Zubavichus, Yu.L. Slovokhotov, P.J. Schilling, R.C. Tittsworth, A.S. Golub, G.A. Protzenko, Inorg. Chim. Acta 280 (1998) 211.
[93] F. Wypych, Th. Weber, R. Prins, Surf. Sci. 32 (1997) L474.
[94] F. Wypych, Th. Weber, R. Prins, Chem. Mater. 10 (1998) 723.
[95] J. Heising, M.G. Kanatzidis, J. Am. Chem. Soc. 121 (1999) 11720.
[96] J. Heising, M.G. Kanatzidis, J. Am. Chem. Soc. 121 (1999) 638.
[97] J.J. Bertzelius, Traité de Chimie, Firman Didot Frères, Paris, 1830.
[98] F.T. Eggertsen, R.M. Roberts, J. Am. Chem. Soc. 63 (1959) 1981.
[99] W.H. Pan, M.E. Leonowicz, E.I. Stiefel, Inorg. Chem. 22 (1983) 672.
[100] A. Müller, W.O. Nolte, B. Krebs, Inorg. Chem. 19 (1980) 2835.
[101] J.L. Brito, M. Ilija, P. Hernández, Thermochim. Acta 256 (1995) 325.
[102] P. Afanasiev, I. Bezverkhyy, Appl. Catal. 322 (2007) 129.
[103] R.I. Walton, A.J. Dent, S.J. Hibble, Chem. Mater. 10 (1998) 3737.
[104] D. Genuit, P. Afanasiev, M. Vrinat, J. Catal. 235 (2005) 302.
[105] A. Müller, E. Diemann, A. Branding, F.W. Baumann, M. Breysse, M. Vrinat, Appl. Catal. 63 (1990) L13.
[106] T.P. Prasad, E. Diemann, A. Müller, J. Inorg. Nucl. Chem. 35 (1973) 1895.
[107] A.M.A. Müller, E. Diemann, Chimia 39 (1985) 312.
[108] E. Diemann, A. Müller, P.R. Aymonino, Z. Anorg. Allg. Chem. 479 (1981) 191.
[109] A. Leist, S. Stauf, S. Löken, E.W. Finckh, S. Lüdtke, K.K. Unger, W. Assenmacher, W. Mader, W. Tremel, J. Mater. Chem. 8 (1998) 241.
[110] D. Genuit, I. Bezverkhyy, P. Afanasiev, J. Solid State Chem. 178 (2005) 2759.
[111] N. Rueda, R. Bacaud, M. Vrinat, J. Catal. 169 (1997) 404.
[112] G. Alonso, M. Del Valle, J. Cruz, A. Licea-Claverie, V. Petranovskii, S. Fuentes, Catal. Lett. 52 (1998) 55.
[113] Y. Yoneyama, C. Song, Catal. Today 50 (1999) 19.
[114] R.R. Chianelli, T.A. Pecoraro, U.S. Patent, 4,288,422, 1981.
[115] D. Nicosia, R. Prins, J. Catal. 229 (2005) 424.
[116] C. Glasson, C. Geantet, M. Lacroix, F. Labruyere, P. Dufresne, J. Catal. 212 (2002) 76.
[117] G. Alonso, G. Aguirre, I.A. Rivero, S. Fuentes, Inorg. Chim. Acta 274 (1998) 108.
[118] R. Frety, M. Breysse, M. Lacroix, M. Vrinat, Bull. Soc. Chim. Belg. 93 (1984) 663.
[119] K. Ramanathan, S. Weller, J. Catal. 95 (1985) 249.
[120] Y. Iwata, K. Sato, T. Yoneda, Y. Miki, Y. Sugimoto, A. Nishijima, Catal. Today 45 (1998) 353.
[121] E. Frommell, J. Diehl, J. Tamilia, S. Pollack, in: Proceedings of 12th North American Meeting of Catalytic Society, Lexington, KY, 1991 (PD-38).
[122] G. Alonso, M. Del Valle, J. Cruz, V. Petranovskii, A. Licea-Claverie, S. Fuentes, Catal. Today 43 (1998) 117.
[123] R.R. Chianelli, G. Berhault, Catal. Today 53 (1999) 357.
[124] M.H. Siadati, G. Alonso, B. Torres, R.R. Chianelli, Appl. Catal. A 305 (2006) 160.
[125] M. Bockrath, D.H. Cobden, J. Lu, A.G. Rinzler, R.E. Smalley, L. Balents, P.L. McEuen, Nature 397 (1999) 598.
[126] A. Bachtold, C. Strunk, J.P. Salvetat, J.M. Bonard, L. Forro, T. Nussbaumer, C. Schonenberger, Nature 389 (1999) 582.
[127] A.L. Ivanovskii, Russ. Chem. Rev. 68 (1999) 103.
[128] M.M.J. Treacy, T.W. Ebbesen, J.M. Gibson, Nature 381 (1996) 678.
[129] P. Bourdieu, Les usages sociaux de la science pour une sociologie clinique du champ scientifique: une conférence-débat, Paris, 11 mars 1997, INRA Editions, 1997.
[130] R. Tenne, L. Margulis, M. Genut, G. Hodes, Nature 360 (1992) 444.
[131] R. Tenne, Adv. Mater. 7 (1995) 965.
[132] R. Tenne, Angew. Chem. Int. Ed. 42 (2003) 5124.
[133] M. Remskar, Adv. Mater. 16 (2004) 1497.
[134] M. Remskar, Z. Skraba, R. Sanjines, F. Levy, Appl. Phys. Lett. 74 (1999) 633.
[135] M. Chhowalla, G.A.J. Amaratunga, Nature 407 (2000) 164.
[136] A. Zak, Y. Feldman, V. Alperovich, R. Rosentsveig, R. Tenne, J. Am. Chem. Soc. 122 (2000) 11108.
[137] Y. Feldman, G.L. Frey, M. Homyonfer, V. Lyakhovitskaya, L. Margulis, H. Cohen, G. Hodes, J.L. Hutchison, R. Tenne, J. Am. Chem. Soc. 118 (1996) 5362.
[138] M. Remskar, Z. Skraba, F. Cleton, R. Sanjines, F. Levy, Appl. Phys. Lett. 69 (1996) 351.
[139] M. Remskar, Z. Skraba, F. Cleton, R. Sanjines, F. Levy, Surf. Rev. Lett. 5 (1998) 423.
[140] W.K. Hsu, B.H. Chang, Y.Q. Zhu, W.Q. Han, H. Terrones, M. Terrones, N. Grobert, A.K. Cheetham, H.W. Kroto, D.R.M. Walton, J. Am. Chem. Soc. 122 (2000) 10155.
[141] P.A. Parilla, A.C. Dillon, K.M. Jones, G. Riker, D.L. Schulz, D.S. Ginley, M.J. Heben, Nature 397 (1999) 144.
[142] M. Bar-Sadan, A.N. Enyashin, S. Gemming, R. Popovitz-Biro, S.Y. Hong, Yehiam Prior, R. Tenne, G. Seifert, J. Phys. Chem. B 110 (2006) 25399.
[143] M. Remskar, A. Mrzel, Z. Skraba, A. Jesih, M. Ceh, J. Demsÿar, P. Stadelmann, F. Levy, D. Mihailovic, Science 292 (2001) 479.
[144] D. Vollath, D.V. Szabó, Mater. Lett. 35 (1998) 236.
[145] E. Devers, P. Afanasiev, B. Jouguet, M. Vrinat, Catal. Lett. 82 (2002) 13.
[146] R.R. Chianelli, M. Daage, M.J. Ledoux, Adv. Catal. 40 (1994) 177.
[147] Y. Peng, Z. Meng, C. Zhong, J. Lu, W. Yu, Z. Yang, Y. Qian, J. Solid State Chem. 159 (2001) 170.
[148] X. Bokhimi, J.A. Toledo, J. Navarrete, X.C. Sun, M. Portilla, Int. J. Hydrogen Energy 26 (2001) 1271.
[149] W.J. Li, E.W. Shi, J.M. Ko, Z. Chen, H. Ogino, T. Fukuda, J. Cryst. Growth 250 (2003) 418.
[150] Q. Li, M. Li, Z. Chen, C. Li, Mater. Res. Bull. 39 (2004) 981.
[151] Y. Tian, Y. He, Y. Zhu, Mater. Chem. Phys. 87 (2004) 87.
[152] Y. Peng, Z. Meng, C. Zhong, J. Lu, Z. Yang, Y. Qian, Mater. Chem. Phys. 73 (2002) 327.
[153] R.R. Chianelli, E.B. Prestridge, J.P. De NeufVille, Science 203 (1979) 1105.
[154] I. Bezverkhy, P. Afanasiev, M. Lacroix, Inorg. Chem. 39 (2000) 5416.
[155] I. Bezverkhyy, P. Afanasiev, C. Geantet, M. Lacroix, J. Catal. 204 (2001) 495.
[156] I. Bezverkhyy, P. Afanasiev, M. Lacroix, J. Catal. 230 (2005) 133.
[157] P. Afanasiev, C. Geantet, C. Thomazeau, B. Jouguet, Chem. Commun. (2000) 1001.
[158] P. Afanasiev, I. Bezverkhy, J. Phys. Chem. B 107 (2003) 2678.

[159] G.B. Saupe, C.C. Waraksa, H.N. Kim, Y.J. Han, D.M. Kaschak, D.M. Skinner, T.E. Mallouk, Chem. Mater. 12 (2000) 1556.
[160] M. Adachi, T. Harada, M. Harada, Langmuir 16 (2000) 2376.
[161] Z. Meng, Y. Peng, Y. Qian, Chem. Commun. (2001) 469.
[162] S. Chiruvolu, H.E. Warriner, E. Naranjo, S.H.J. Idziak, J.O. Radler, R.J. Plano, J.A. Zasadinski, C.R. Safinya, Science 266 (1994) 1222.
[163] J.L. Israelachvili, J.D. Mitchell, W.B. Niham, J. Chem. Soc., Faraday Trans. 272 (1976) 1525.
[164] B.H. Robinson, S. Bucak, A. Fontana, Langmuir 16 (2000) 8231.
[165] F.J. Carrion, A. de la Maza, J.L. Parra, J. Colloid Interface Sci. 164 (1994) 78.
[166] H. Liao, Y. Wang, S. Zhang, Y. Qian, Chem. Mater. 13 (2001) 6.
[167] P. Afanasiev, G.-F. Xia, G. Berhault, B. Jouguet, M. Lacroix, Chem. Mater. 11 (1999) 3216.
[168] Y. Xiong, Y. Xie, Z. Li, X. Li, R. Zhang, Chem. Phys. Lett. 382 (2003) 180.
[169] Y. Wang, J.-S. Chen, M.-H. Xin, R.-R. Xu, Inorg. Chem. Commun. 3 (1999) 129.
[170] I. Bezverkhyy, P. Afanasiev, M. Lacriox, Mater. Res. Bull. 37 (2002) 161.
[171] P.N. Trikalitis, T.A. Kerr, M.G. Kanatzidis, Microporous Mesoporous Mater. 88 (2005) 187.
[172] L.F. Flores-Ortiz, M.A. Cortés-Jácome, C. Ángeles-Chávez, J.A. Toledo-Antonio, Sol. Energy Mater. Sol. Cells 90 (2006) 813.
[173] E.A. Ponomarev, M. Neumann-Spallart, G. Hodes, C. Lévy-Clément, Thin Solid Films 280 (1996) 86.
[174] H.J. Bykcr, A.E. Austin 160th Electrochem. Soc. Meeting, abstract, J. Electrochem. Soc. 128 (1981) 381C.
[175] A. Albu-Yaron, C. Levy-Clement, J.L. Hutchison, Electrochem. Solid-State Lett. 2 (1999) 627.
[176] M.S. Donley, N.T. McDevitt, T.W. Haas, P.T. Murray, J.T. Grant, Thin Solid Films 168 (1989) 335.
[177] M.S. Donley, P.T. Murray, S.A. Barber, T.W. Haas, Surf. Coat. Technol. 36 (1988) 329.
[178] G. Chatzitheodorou, S. Fiechter, M. Kunst, J. Luck, H. Tributsch, Mater. Res. Bull. 23 (1988) 1261.
[179] W.K. Hoffman, J. Mater. Sci. 23 (1988) 3981.
[180] J. Cheon, J.E. Gozum, G.S. Girolami, Chem. Mater. 9 (1997) 1847.
[181] O.C. Monteiro, T. Trindade, Mater. Res. Bull. 39 (2004) 357.
[182] C. Geantet, D.H. Kerridge, T. Decamp, B. Durand, M. Breysse, Mater. Sci. Forum 73–75 (1991) 693.
[183] P. Afanasiev, L. Rawas, M. Vrinat, Mater. Chem. Phys. 73 (2002) 295.
[184] D. Mahajan, C.L. Marshall, N. Castagnola, J.C. Hanson, Appl. Catal., A 258 (2004) 83.
[185] T. Hyeon, M. Fang, K.S. Suslick, J. Am. Chem. Soc. 118 (1996) 5492.
[186] I. Uzcanga, I. Bezverkhyy, P. Afanasiev, C. Scott, M. Vrinat, Chem. Mater. 17 (2005) 3575.
[187] Y. Iwata, Y. Araki, K. Honna, Y. Miki, K. Sato, H. Shimada, Catal. Today 65 (2001) 335.